

# Interplay of Coulomb interactions and disorder in three dimensional quadratic band crossings without time-reversal or particle-hole symmetry

Ipsita Mandal<sup>1</sup> and Rahul M. Nandkishore<sup>2</sup>

<sup>1</sup>*Department of Physics, Indian Institute of Technology, Kharagpur, 721302 India*

<sup>2</sup>*Department of Physics and Center for Theory of Quantum Matter,  
University of Colorado at Boulder, Boulder, CO 80309, USA*

(Dated: December 14, 2024)

## Abstract

Coulomb interactions famously drive three dimensional quadratic band crossing semimetals into a non-Fermi liquid phase of matter. In a previous work, *Phys. Rev. B* **95**, 205106 (2017) the effect of disorder on this non-Fermi liquid phase was investigated, assuming that the bandstructure was particle-hole symmetric and isotropic, and assuming that the disorder preserved exact time-reversal symmetry and statistical isotropy. It was shown that the non-Fermi liquid fixed point is unstable to disorder, and that a runaway flow to strong disorder occurs. In this work, we extend that analysis by relaxing the twin assumptions of time-reversal and particle-hole symmetry (but continuing to assume isotropy of the low energy bandstructure). We first incorporate time-reversal symmetry breaking disorder, and demonstrate that there do not appear any new fixed points. Moreover, while the system continues to flow to strong disorder, time-reversal-symmetry-breaking disorder grows asymptotically more slowly than time-reversal-symmetry-preserving disorder, which we therefore expect should dominate the strong-coupling phase. We then introduce a perturbation that breaks the particle-hole symmetry of the bandstructure. We show that whereas this perturbation is *irrelevant* in the clean system, it is *relevant* in the presence of disorder, such that the ‘effective masses’ of the conduction and valence bands should become sharply distinct in the low-energy limit. We calculate the RG flow equations for the disordered interacting system in the presence of particle-hole symmetry breaking in the bandstructure, and demonstrate that the problem exhibits a runaway flow to strong disorder. Along the runaway flow, time-reversal-symmetry-preserving disorder grows asymptotically more rapidly than both time-reversal-symmetry-breaking disorder and the Coulomb interaction.

## CONTENTS

|  |    |
|--|----|
| I. Introduction  | 3  |
| II. Model  | 3  |
| A. Action  | 4  |
| B. Scaling dimensions and RG scheme  | 5  |
| III. Including time-reversal symmetry breaking disorder  | 6  |
| A. Addition of the $W_2$ vertex to the non-interacting problem   | 8  |
| 1. Fermion self-energy   | 8  |
| 2. ZS diagrams   | 8  |
| 3. VC diagrams   | 9  |
| 4. BCS and ZS' diagrams  | 10 |
| 5. RG equations  | 11 |
| B. Addition of the $W_2$ vertex in the presence of Coulomb interactions  | 12 |
| 1. ZS diagram  | 12 |
| 2. VC diagrams   | 13 |
| 3. BCS and ZS' diagrams  | 13 |
| C. RG equations  | 13 |
| D. Strong-coupling trajectories  | 14 |
| IV. Particle-hole symmetry breaking in the bandstructure   | 16 |
| A. Renormalization of the particle-hole symmetry-breaking term   | 17 |
| B. Recomputing $\beta$ functions with particle-hole-asymmetric bandstructure   | 19 |
| 1. Clean system  | 19 |
| 2. Disordered non-interacting system   | 20 |
| 3. Disordered interacting problem  | 20 |
| C. RG equations  | 21 |
| D. Strong-coupling trajectories  | 23 |
| V. Analysis and discussion   | 25 |
| A. Clifford algebra and various identities   | 26 |
| B. Vanishing divergent contributions from the VC, BCS, ZS' diagrams in the clean system with $\frac{k^2}{2m'}$ term. | 27 |
| References   | 28 |

## I. INTRODUCTION

In 1971 Abrikosov studied isotropic three dimensional systems with *quadratic* band crossings using a renormalization group calculation in  $4 - \varepsilon$  dimensions [1], and argued that Coulomb interactions could stabilize a *non-Fermi liquid* phase. Interest in this problem has recently been revived [2–6] because of its relevance for pyrochlore iridates. However, theoretical explorations have largely been confined to the *clean* (disorder-free) problem, whereas realistic materials are always disordered to some degree. The interplay of disorder with Coulomb interactions in three dimensional quadratic band crossings is a particularly rich problem, since both disorder and Coulomb interactions are *relevant* with the *same* scaling dimension, and thus should be treated on an equal footing.

In two recent works [7, 8] the interplay of disorder and Coulomb interactions was investigated, assuming (a) exact time-reversal symmetry (b) particle-hole (PH) symmetry of the bandstructure and (c) isotropy. It was shown that disorder is a relevant perturbation to Abrikosov’s non-Fermi liquid fixed point, and that the disordered problem undergoes a runaway flow to strong disorder, the implications of which were discussed at length in [8]. In this work, we extend the analysis (working with the renormalization group scheme of [8]) to incorporate time-reversal symmetry breaking disorder, as well as terms in the band-structure that break PH symmetry (while preserving isotropy). We have used the powerful technique of dimensional regularization, which has been successfully used in many problems involving non-fermi liquids [9, 10].

This paper is structured as follows. In Sec. II we introduce the basic model and renormalization group scheme. In Sec. III we calculate the interplay of interactions and disorder, including time-reversal symmetry breaking ‘tensor’ disorder which was ignored in previous analyses. We show that no new fixed points appear, and the problem continues to flow to strong disorder. We further show that time-reversal symmetry breaking disorder grows asymptotically more slowly than time-reversal symmetry preserving disorder as the problem flows to strong disorder. In Sec. IV we further relax the assumption of PH symmetry of the band-structure. Our analysis of the  $\beta$  functions, and discussion of the results, is presented in Sec. V. The appendices contain technical results employed in the derivations, but which are inessential to the flow of the argument.

## II. MODEL

We consider a model for three-dimensional quadratic band crossings, where the low energy bands form a four-dimensional representation of the lattice symmetry group [2]. Then the  $\mathbf{k} \cdot \mathbf{p}$  Hamiltonian for the non-interacting system, in the absence of disorder, takes the form [3]:

$$\mathcal{H}_0 = \sum_{a=1}^N d_a(\mathbf{k}) \Gamma_a + \frac{k^2}{2m'}, \quad d_a(\mathbf{k}) = \frac{\tilde{d}_a(\mathbf{k})}{2m}, \quad (2.1)$$

where the  $\Gamma_a$ 's are the rank four irreducible representations of the Clifford algebra relation  $\{\Gamma_a, \Gamma_b\} = 2\delta_{ab}$  in the Euclidean space. We have used the usual notation  $\{A, B\} = AB + BA$  for denoting the anticommutator. There are  $N = 5$  such matrices, which are related to the familiar gamma matrices from the Dirac equation (plus the matrix conventionally denoted as  $\gamma_5$ ), but with the Euclidean metric  $\{\Gamma_a, \Gamma_b\} = 2\delta_{ab}$  instead of the Minkowski metric  $\{\Gamma_a, \Gamma_b\} = 2(-1, +1, +1, +1)$ . Using various Clifford algebra relations, as shown in Appendix A. In  $d = 3$ , the space of  $4 \times 4$  Hermitian matrices is spanned by the identity matrix, the five  $4 \times 4$  Gamma matrices  $\Gamma_a$  and the ten distinct matrices  $\Gamma_{ab} = \frac{1}{2i} [\Gamma_a, \Gamma_b]$ . Furthermore, the  $\tilde{d}_a(k)$ 's are the  $l = 2$  spherical harmonics, which have the following structure:

$$\begin{aligned} \tilde{d}_1(\mathbf{k}) &= \sqrt{3} k_y k_z, & \tilde{d}_2(\mathbf{k}) &= \sqrt{3} k_x k_z, & \tilde{d}_3(\mathbf{k}) &= \sqrt{3} k_x k_y, \\ \tilde{d}_4(\mathbf{k}) &= \frac{\sqrt{3}(k_x^2 - k_y^2)}{2}, & \tilde{d}_5(\mathbf{k}) &= \frac{2k_z^2 - k_x^2 - k_y^2}{2}. \end{aligned} \quad (2.2)$$

The isotropic  $\frac{k^2}{2m^*}$  term with no spinor structure introduces particle-hole asymmetry to the band-structure. This is an irrelevant perturbation in the clean system [1], and was ignored in previous analyses [7, 8]. We consider a setting with  $N_f$  independent flavours of fermions.

### A. Action

The full action, following the arguments and notations in Ref. [8], is given by:

$$\begin{aligned} S &= \sum_{i, \xi} \int d\tau d^d x \psi_i^{\xi\dagger}(x, \tau) [\partial_\tau - \mathcal{H}_0(x)] \psi_i^\xi(x, \tau) \\ &+ \sum_{i, \xi, \xi'} \frac{e^2}{2c} \int d\tau d^d q d^d p d^d p' V(q) \psi_i^{\xi\dagger}(\mathbf{p}, \tau) \psi_i^{\xi'\dagger}(\mathbf{p}', \tau) \psi_i^{\xi'}(\mathbf{p} - \mathbf{q}, \tau) \psi_i^\xi(\mathbf{p} + \mathbf{q}, \tau) \\ &- W_0 \sum_{i, j, \xi} \int d\tau d\tau' d^d x (\psi_i^{\xi\dagger} \psi_i^\xi)_\tau (\psi_j^{\xi\dagger} \psi_j^\xi)_{\tau'} - W_1 \sum_{i, j=1}^n \sum_a \int d\tau d\tau' d^d x (\psi_i^{\xi\dagger} \Gamma_a \psi_i^\xi)_\tau (\psi_j^{\xi\dagger} \Gamma_a \psi_j^\xi)_{\tau'} \\ &- W_2 \sum_{i, j, \xi} \sum_{a < b} \int d\tau d\tau' d^d x (\psi_i^{\xi\dagger} \Gamma_{ab} \psi_i^\xi)_\tau (\psi_j^{\xi\dagger} \Gamma_{ab} \psi_j^\xi)_{\tau'}, \end{aligned} \quad (2.3)$$

where the Coulomb interaction  $V(q) = \frac{1}{q^2}$  has been written in momentum space, and  $\xi = (1, 2, \dots, N_f)$  (same with  $\xi'$ ) denotes the flavour index. Note that disorder has been taken to be diagonal in the flavor space. The disorder terms, parametrized by the constants  $W_\alpha$  ( $\alpha = 0, 1, 2$ ), represent short-range-correlated disorder with and without spinor structure. The disorder is treated in the replica formalism with replica indices  $i, j$ , with  $n$  replicas  $n$ . The limit  $n \rightarrow 0$  has to be taken at the end of the computation. The sums over  $a$  range over all the five independent  $4 \times 4$  non-identity Hermitian matrices  $\Gamma_a$  in the spinor space, while the sums over  $(a, b)$  range over all the ten independent matrices  $\Gamma_{ab}$ . Furthermore, the short-ranged interactions have been neglected as

they are less relevant in an RG sense, compared to either the long-ranged (Coulomb) interactions or short-range-correlated disorder.

The Hamiltonian in Eq. (2.1), in the absence of the  $\frac{k^2}{2m'}$  term, has been considered in the presence of “scalar” (disorder vertex contains no gamma matrix) and “vector” (disorder vertex contains one gamma matrix) disorder terms, in the absence and presence of the Coulomb interaction, in Ref. [8]. In Sec. III of the present work we generalize the analysis to include time reversal symmetry breaking ‘tensor’ disorder ( $W_2 \neq 0$ ). Meanwhile, the  $\frac{k^2}{2m'}$  term was dropped in Ref. [8] as it is irrelevant in the  $\mathbf{k} \cdot \mathbf{p}$  Hamiltonian in the presence of Coulomb interactions [1, 2] for the clean system. In Sec. IV we re-introduce this term, and analyze the interplay of all kinds of disorder and Coulomb interactions allowing for particle-hole asymmetry in the bandstructure.

## B. Scaling dimensions and RG scheme

The canonical scaling dimensions are given by:  $[x^{-1}] = 1$  and  $[\tau^{-1}] = z$  (dynamical critical exponent). From the invariance of the bare action, we find that  $[\psi^\xi] = d/2$  and  $[m] = [m'] = 2 - z$  in  $d$  spatial dimensions, where  $z = 2$  at tree level. For the Coulomb and disorder terms, we get:

$$[e^2] = z + 2 - d \quad [W_\alpha] = 2z - d - 2\eta_\alpha, \quad (2.4)$$

where we have allowed for the anomalous exponents  $[\tilde{\psi}^\dagger \tilde{\psi}] = d + \eta_0$ ,  $[\tilde{\psi}^\dagger \Gamma_a \tilde{\psi}] = d + \eta_1$  and  $[\tilde{\psi}^\dagger \Gamma_{ab} \tilde{\psi}] = d + \eta_2$ . The anomalous exponents are zero at the Gaussian fixed point, and hence all the  $W_\alpha$ 's have the same tree-level scaling. Since both the Coulomb interactions and disorder are relevant at tree level with the *same* exponent, at least at the Gaussian fixed point about which the perturbation is being carried out, they must be treated on an equal footing.

Our RG scheme involves a continuation to  $d = 4 - \varepsilon$  dimensions, as in  $d = 4$ , the Coulomb interaction and disorder are marginal at tree level<sup>1</sup>. We need to combine this with the RG scheme developed by Moon *et al* [2] due to reasons explained in Ref. [8], which involves continuing to four spatial dimensions while assuming that the angular and gamma matrix structures remain the same as in  $d = 3$ . This implies that the radial momentum integrals are performed with respect to a  $d = 4 - \varepsilon$  dimensional measure  $\int \frac{p^{3-\varepsilon} dp}{(2\pi)^{4-\varepsilon}}$ , but angular momentum integrals are performed only over the three-dimensional sphere parametrized by the polar and azimuthal angles  $(\theta, \varphi)$ . Nevertheless, the overall angular integral of an isotropic function  $\int_{\Omega} \cdot 1$  is taken to be  $2\pi^2$  (as is appropriate for the total solid angle in  $d = 4$ ), and the angular integrals are normalized accordingly. Therefore, the angular integrations are performed with respect to the measure

$$\int dS(\dots) \equiv \frac{\pi}{2} \int_0^\pi d\theta \int_0^{2\pi} d\varphi \sin\theta(\dots), \quad (2.5)$$

<sup>1</sup> However, a description of the physical situation requires a continuation to  $\varepsilon = 1$ , which could be problematic [3].



FIG. 1. These two diagrams determine the  $O(\varepsilon)$  correction to the Green's function with each solid line representing the bare Green function. A dashed line may represent either a disorder or the Coulomb interaction. If the dashed line represents disorder, then it connects two fermion lines at the same point in real space, but they may have different time and replica indices. For disorder interaction, the diagram (b) is then proportional to the number of replica flavours  $n$ , and vanishes upon taking the replica limit  $n \rightarrow 0$ . If the dashed line represents the Coulomb interaction, then it connects two fermions with the same time index and same replica index, but with different spatial positions.

where the  $\pi/2$  is inserted for the sake of normalization. For performing the angular integrals, we will use the notation

$$\hat{d}_a(\mathbf{k}) = \frac{\tilde{d}_a(\mathbf{k})}{k^2}, \quad (2.6)$$

such that

$$\int dS \hat{d}_a(\mathbf{k}) = 0, \quad \int dS \hat{d}_a(\mathbf{k}) \hat{d}_b(\mathbf{k}) = \frac{2\pi^2 \delta_{ab}}{N}. \quad (2.7)$$

We note that  $|\mathbf{d}(\mathbf{k})|^2 = \frac{k^4}{4m^2}$ .

We will consider RG flows by considering the one-loop corrections coming from the diagrams shown in Figs 1 and 2. We will employ the momentum-shell RG and take  $\Lambda_{\text{UV}} = \Lambda_{\text{IR}} e^{-l}$ , where  $\Lambda_{\text{UV}}$  ( $\Lambda_{\text{IR}}$ ) is the UV (IR) cut-off for the energy/momentum integrals and  $l$  is the logarithmic length scale. We will use the one-loop  $\beta$  functions, that dictate the flow of the parameters with increasing  $l$ . Furthermore, in our RG scheme we will hold  $m$  fixed, i.e.  $m$  does not flow such that

$$\frac{dm}{dl} = 0. \quad (2.8)$$

### III. INCLUDING TIME-REVERSAL SYMMETRY BREAKING DISORDER

In this section we incorporate time-reversal symmetry breaking disorder, while continuing to assume that the bandstructure is PH symmetric. In the absence of the  $\frac{k^2}{2m'}$  term, the bare Green's function for each fermionic flavour is given by:

$$G_0(\omega, \mathbf{k}) = \frac{1}{-i\omega + \mathbf{d}(\mathbf{k}) \cdot \mathbf{\Gamma}} = \frac{i\omega + \mathbf{d}(\mathbf{k}) \cdot \mathbf{\Gamma}}{\omega^2 + |\mathbf{d}(\mathbf{k})|^2}, \quad (3.1)$$

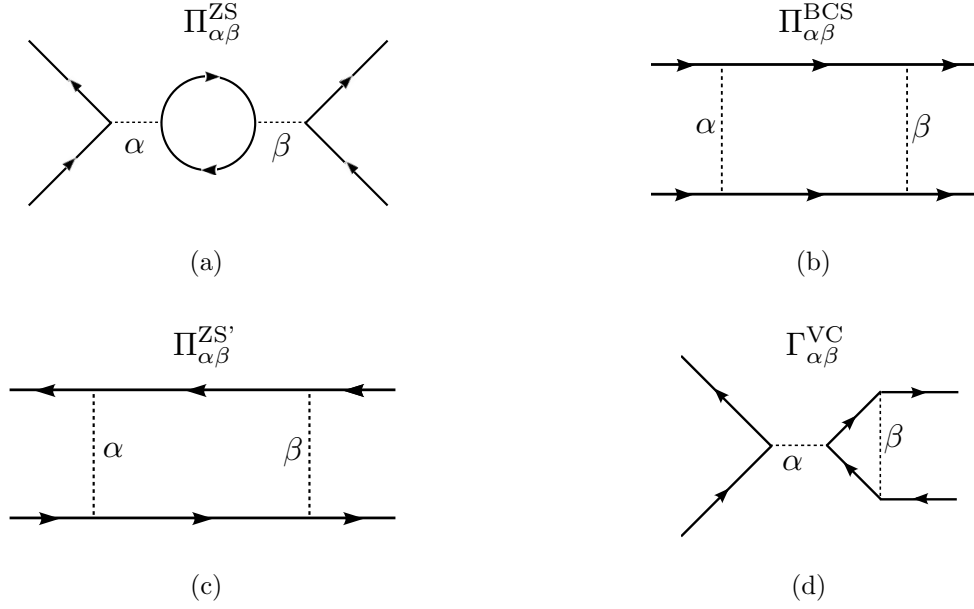


FIG. 2. These diagrams determine the  $O(\varepsilon)$  correction to the four-fermion vertices (either disorder or interaction) and are denoted by ZS, BCS, ZS' and VC, respectively, following the convention of Ref. [11]. Each solid line represents the bare Green function. A dashed line may represent either a disorder or the Coulomb interaction. Note that unlike the ZS, BCS, and ZS' diagrams, the VC diagrams are generically not symmetric under interchange of indices, *i.e.*  $\Gamma_{\alpha\beta}^{\text{VC}} \neq \Gamma_{\beta\alpha}^{\text{VC}}$ .

here  $|d(\mathbf{k})|^2 = (\frac{k^2}{2m})^2$ . The Abrikosov fixed point for the clean system is given by:

$$u = u^* \equiv \frac{15}{2(4 + 15 N_f)}, \quad \text{where } u = \frac{m e^2}{8 \pi^2 c}. \quad (3.2)$$

All diagrams not involving  $W_2$  lines were computed in [8]. Our immediate challenge is to augment that analysis with time-reversal symmetry breaking disorder,  $W_2 \neq 0$

## A. Addition of the $W_2$ vertex to the non-interacting problem

The loop corrections to the disorder lines themselves come from the fully connected contractions of

$$\begin{aligned}
\delta S = \frac{1}{2} \int d\tau d\tau' d\tau'' d\tau''' d^d x d^d x' \sum_{i,j,k,l,\xi} & \left[ W_0^2 (\psi_i^{\xi\dagger} \psi_i^\xi)_x^\tau (\psi_j^{\xi\dagger} \psi_j^\xi)_{x'}^{\tau'} (\psi_k^{\xi\dagger} \psi_k^\xi)_{x''}^{\tau''} (\psi_l^{\xi\dagger} \psi_l^\xi)_{x'''}^{\tau'''} \right. \\
& + W_1^2 (\psi_i^{\xi\dagger} \Gamma_a^i \psi_i^\xi)_x^\tau (\psi_j^{\xi\dagger} \Gamma_a^j \psi_j^\xi)_{x'}^{\tau'} (\psi_k^{\xi\dagger} \Gamma_b^k \psi_k^\xi)_{x''}^{\tau''} (\psi_l^{\xi\dagger} \Gamma_b^l \psi_l^\xi)_{x'''}^{\tau'''} \\
& + 2 W_0 W_1 (\psi_i^{\xi\dagger} \psi_i^\xi)_x^\tau (\psi_j^{\xi\dagger} \psi_j^\xi)_{x'}^{\tau'} (\psi_k^{\xi\dagger} \Gamma_b^k \psi_k^\xi)_{x''}^{\tau''} (\psi_l^{\xi\dagger} \Gamma_b^l \psi_l^\xi)_{x'''}^{\tau'''} \\
& + W_2^2 (\psi_i^{\xi\dagger} \Gamma_{ab}^i \psi_i^\xi)_x^\tau (\psi_j^{\xi\dagger} \Gamma_{ab}^j \psi_j^\xi)_{x'}^{\tau'} (\psi_k^{\xi\dagger} \Gamma_{cd}^k \psi_k^\xi)_{x''}^{\tau''} (\psi_l^{\xi\dagger} \Gamma_{cd}^l \psi_l^\xi)_{x'''}^{\tau'''} \\
& + 2 W_0 W_2 (\psi_i^{\xi\dagger} \psi_i^\xi)_x^\tau (\psi_j^{\xi\dagger} \psi_j^\xi)_{x'}^{\tau'} (\psi_k^{\xi\dagger} \Gamma_{cd}^k \psi_k^\xi)_{x''}^{\tau''} (\psi_l^{\xi\dagger} \Gamma_{cd}^l \psi_l^\xi)_{x'''}^{\tau'''} \\
& \left. + +2 W_1 W_2 (\psi_i^{\xi\dagger} \Gamma_a^i \psi_i^\xi)_x^\tau (\psi_j^{\xi\dagger} \Gamma_a^j \psi_j^\xi)_{x'}^{\tau'} (\psi_k^{\xi\dagger} \Gamma_{cd}^k \psi_k^\xi)_{x''}^{\tau''} (\psi_l^{\xi\dagger} \Gamma_{cd}^l \psi_l^\xi)_{x'''}^{\tau'''} \right], \quad (3.3)
\end{aligned}$$

where repeated  $\Gamma$ -matrix indices are as usual summed over, and we have kept track of the replica indices on  $\Gamma$  matrices. We note that we must incorporate  $a \neq b$  ( $c \neq d$ ) for the sum over  $\Gamma_{ab}$  ( $\Gamma_{cd}$ ) matrices as we should consider only the independent terms.

### 1. Fermion self-energy

$$\Sigma_{W_2}(\omega, \mathbf{k}) = 2 W_2 \int \frac{d^d p}{(2\pi)^d} \Gamma_{ab} G(\omega, \mathbf{k}) \Gamma_{ab} = \frac{i \omega m^2 W_2 N (N-1)}{2 \pi^2} \ln \left( \frac{\Lambda_{UV}}{\Lambda_{IR}} \right). \quad (3.4)$$

In the presence of the tensor disorder, the dynamical exponent is modified to:

$$z = 2 + \frac{m^2}{\pi^2} \left[ W_0 + N W_1 + \frac{N(N-1) W_2}{2} \right] = 2 + \frac{\lambda_0 + N \lambda_1 + \frac{N(N-1) \lambda_2}{2}}{2}, \quad (3.5)$$

where

$$\lambda_\alpha = \frac{\pi^2 W_\alpha}{2 m^2} \quad \text{for } \alpha = 0, 1, 2. \quad (3.6)$$

### 2. ZS diagrams

These are zero.

### 3. VC diagrams

A VC with two tensor ( $W_2$ ) lines, emerging from 8 distinct contractions, and after setting the external frequency  $\omega = 0$ , leads to:

$$\begin{aligned}
\frac{\Gamma_{22}^{\text{VC}}}{(2m)^2} &= 4W_2^2 \Gamma_{ab}^i \int \frac{d^d k}{(2\pi)^d} \frac{\Gamma_{cd}^j (\hat{\mathbf{d}}_{\mathbf{k}} \cdot \Gamma^j) \Gamma_{ab}^j (\hat{\mathbf{d}}_{\mathbf{k}} \cdot \Gamma^j) \Gamma_{cd}^j}{k^4} \\
&= \frac{W_2^2 \Gamma_{ab}^i \Gamma_{cd}^j \Gamma_f^j \Gamma_{ab}^j \Gamma_f^j \Gamma_{cd}^j}{2N\pi^2} \ln \left( \frac{\Lambda_{UV}}{\Lambda_{IR}} \right) \\
&= -\frac{W_2^2 (N-4) \Gamma_{ab}^i \Gamma_{cd}^j \Gamma_{ab}^j \Gamma_{cd}^j l}{2N\pi^2} \\
&= -\frac{W_2^2 (N-4) (N^2 - 9N + 12) \Gamma_{ab}^i \Gamma_{ab}^j l}{4N\pi^2}, \tag{3.7}
\end{aligned}$$

using Eq. (A3). The counterterm is thus given by  $\delta\lambda_2 = \frac{(N-4)(N^2-9N+12)}{2N} \lambda_2^2 l$ .

$$\begin{aligned}
\frac{\Gamma_{02}^{\text{VC}}}{(2m)^2} &= 4W_0 W_2 \int \frac{d^d k}{(2\pi)^d} \frac{\Gamma_{cd}^j (\hat{\mathbf{d}}_{\mathbf{k}} \cdot \Gamma^j) (\hat{\mathbf{d}}_{\mathbf{k}} \cdot \Gamma^j) \Gamma_{cd}^j}{k^4} \\
&= \frac{W_0 W_2 \Gamma_{cd}^j \Gamma_f^j \Gamma_f^j \Gamma_{cd}^j}{2N\pi^2} \ln \left( \frac{\Lambda_{UV}}{\Lambda_{IR}} \right) \\
&= -\frac{W_0 W_2 N (N-1) l}{4\pi^2}. \tag{3.8}
\end{aligned}$$

This gives the counterterm  $\delta\lambda_0 = \frac{N(N-1)}{2} \lambda_0 \lambda_2 l$ .

$$\begin{aligned}
\frac{\Gamma_{20}^{\text{VC}}}{(2m)^2} &= 4W_2 W_0 \Gamma_{ab}^i \int \frac{d^d k}{(2\pi)^d} \frac{(\hat{\mathbf{d}}_{\mathbf{k}} \cdot \Gamma^j) \Gamma_{ab}^j (\hat{\mathbf{d}}_{\mathbf{k}} \cdot \Gamma^j)}{k^4} \\
&= \frac{W_2 W_0 \Gamma_{ab}^i \Gamma_f^j \Gamma_{ab}^j \Gamma_f^j}{2N\pi^2} \ln \left( \frac{\Lambda_{UV}}{\Lambda_{IR}} \right) \\
&= -\frac{W_0 W_2 (N-4) \Gamma_{ab}^i \Gamma_{ab}^j l}{2N\pi^2}, \tag{3.9}
\end{aligned}$$

using Eq. (A6). The contribution from this term is thus the counterterm  $\delta\lambda_2 = \frac{N-4}{N} \lambda_0 \lambda_2 l$ .

$$\begin{aligned}
\frac{\Gamma_{12}^{\text{VC}}}{(2m)^2} &= 4W_1 W_2 \Gamma_a^i \int \frac{d^d k}{(2\pi)^d} \frac{\Gamma_{cd}^j (\hat{\mathbf{d}}_{\mathbf{k}} \cdot \Gamma^j) \Gamma_a^j (\hat{\mathbf{d}}_{\mathbf{k}} \cdot \Gamma^j) \Gamma_{cd}^j}{k^4} \\
&= \frac{W_1 W_2 \Gamma_a^i \Gamma_{cd}^j \Gamma_f^j \Gamma_a^j \Gamma_f^j \Gamma_{cd}^j}{2N\pi^2} \ln \left( \frac{\Lambda_{UV}}{\Lambda_{IR}} \right) \\
&= \frac{W_1 W_2 (2-N) \Gamma_a^i \Gamma_{cd}^j \Gamma_a^j \Gamma_{cd}^j}{2N\pi^2} \ln \left( \frac{\Lambda_{UV}}{\Lambda_{IR}} \right) \\
&= \frac{W_1 W_2 (N-1)(N-2)(N-4) \Gamma_a^i \Gamma_a^j l}{4N\pi^2}, \tag{3.10}
\end{aligned}$$

where we have used Eq. (A4). This gives the counterterm  $\delta\lambda_1 = -\frac{(N-1)(N-2)(N-4)}{2N} \lambda_1 \lambda_2 l$ .

$$\begin{aligned}
\frac{\Gamma_{21}^{\text{VC}}}{(2m)^2} &= 4W_2 W_1 \Gamma_{ab}^i \int \frac{d^d k}{(2\pi)^d} \frac{\Gamma_c^j (\hat{\mathbf{d}}_{\mathbf{k}} \cdot \Gamma^j) \Gamma_{ab}^j (\hat{\mathbf{d}}_{\mathbf{k}} \cdot \Gamma^j) \Gamma_c^j}{k^4} \\
&= \frac{W_2 W_1 \Gamma_{ab}^i \Gamma_c^j \Gamma_f^j \Gamma_{ab}^j \Gamma_f^j \Gamma_c^j}{2N\pi^2} \ln \left( \frac{\Lambda_{UV}}{\Lambda_{IR}} \right) \\
&= -\frac{W_1 W_2 (N-4)^2 \Gamma_{ab}^i \Gamma_{ab}^j l}{2N\pi^2}, \tag{3.11}
\end{aligned}$$

using Eq. (A6). The counterterm from this term is  $\delta\lambda_2 = \frac{(N-4)^2}{N} \lambda_1 \lambda_2 l$ .

#### 4. BCS and ZS' diagrams

$$\begin{aligned}
\frac{\Pi_{22}^{\text{BCS}}}{(2m)^2} &= 2W_2^2 \int \frac{d^d k}{(2\pi)^d} \frac{\left[ \Gamma_{ab}^i (\hat{\mathbf{d}}_{\mathbf{k}} \cdot \Gamma^i) \Gamma_{cd}^i \right] \left[ \Gamma_{cd}^j (\hat{\mathbf{d}}_{\mathbf{k}} \cdot \Gamma^j) \Gamma_{ab}^j \right]}{k^4}, \\
\frac{\Pi_{22}^{\text{ZS}'}}{(2m)^2} &= 2W_2^2 \int \frac{d^d k}{(2\pi)^d} \frac{\left[ \Gamma_{ab}^i (\hat{\mathbf{d}}_{\mathbf{k}} \cdot \Gamma^i) \Gamma_{cd}^i \right] \left[ \Gamma_{ab}^j (\hat{\mathbf{d}}_{\mathbf{k}} \cdot \Gamma^j) \Gamma_{cd}^j \right]}{k^4}. \tag{3.12}
\end{aligned}$$

Adding these together, we get:

$$\frac{\Pi_{22}^{\text{BCS}}}{(2m)^2} + \frac{\Pi_{22}^{\text{ZS}'}}{(2m)^2} = \frac{W_2^2}{4N\pi^2} \ln \left( \frac{\Lambda_{UV}}{\Lambda_{IR}} \right) \Gamma_{ab}^i \Gamma_f^i \Gamma_{cd}^i (\Gamma_{cd}^j \Gamma_f^j \Gamma_{ab}^j + \Gamma_{ab}^j \Gamma_f^j \Gamma_{cd}^j) = -\frac{W_2^2 (N-1)! l}{8\pi^2}, \tag{3.13}$$

which corrects the scalar disorder term. The counterterm for this is  $\delta\lambda_0 = \frac{(N-1)!}{4} \lambda_2^2 l$ .

| Coupling    | $\lambda_0$   | $\lambda_1$   | $\lambda_2$   | $u$  |
|-------------|---|---|---|--|
| $\lambda_0$ | $\delta\lambda_0 = \lambda_0^2 l$                       | $\delta\lambda_1 = -\frac{N-2}{N} \lambda_0 \lambda_1 l$    | $\delta\lambda_2 = \frac{N(N-1)}{2} \lambda_0 \lambda_2 l$            | 0  |
| $\lambda_1$ | $\delta\lambda_0 = N \lambda_0 \lambda_1 l$             | $\delta\lambda_1 = \frac{(N-2)^2}{N} \lambda_1^2 l$         | $\delta\lambda_2 = -\frac{(N-1)(N-2)(N-4)}{2N} \lambda_1 \lambda_2 l$ | $\delta\lambda_1 = \frac{2(N-1)}{N} \lambda_1 u l$ |
| $\lambda_2$ | $\delta\lambda_2 = \frac{N-4}{N} \lambda_0 \lambda_2 l$ | $\delta\lambda_2 = \frac{(N-4)^2}{N} \lambda_1 \lambda_2 l$ | $\delta\lambda_2 = \frac{(N-4)(N^2-9N+12)}{2N} \lambda_2^2 l$         | $d\lambda_2 = \frac{4}{N} \lambda_2 u l$           |
| $u$         | $\delta u = \lambda_0 u l$                              | $\delta u = N \lambda_1 u l$                                | $\delta u = \frac{N(N-1)}{2} \lambda_2 u l$                           | 0  |

TABLE I. Contributions to the  $\beta$ -functions from the VC diagrams without the  $\frac{k^2}{2m'}$  term. Here,  $\lambda_\alpha = \frac{2m^2 W_\alpha}{\pi^2}$ ,  $u = \frac{m e^2}{8\pi^2 c}$ , and  $l$  is the RG flow parameter. Terms not involving  $W_2$  are taken from Ref.[8]

$$\begin{aligned}
\frac{\Pi_{02}^{\text{BCS}}}{(2m)^2} + \frac{\Pi_{02}^{\text{ZS}'}}{(2m)^2} &= 4W_0 W_2 \int \frac{d^d k}{(2\pi)^d} \sum_{a<b} \frac{[\Gamma_{ab}^i(\hat{\mathbf{d}}_{\mathbf{k}} \cdot \mathbf{\Gamma}^i)] [\Gamma_{ab}^j(\hat{\mathbf{d}}_{\mathbf{k}} \cdot \mathbf{\Gamma}^j) + (\hat{\mathbf{d}}_{\mathbf{k}} \cdot \mathbf{\Gamma}^j) \Gamma_{ab}^j]}{k^4} \\
&= \frac{W_0 W_2}{4N\pi^2} \ln\left(\frac{\Lambda_{UV}}{\Lambda_{IR}}\right) \sum_{a \neq b, f} \Gamma_{ab}^i \Gamma_f^i (\Gamma_{ab}^j \Gamma_f^j + \Gamma_f^j \Gamma_{ab}^j) \\
&= -\frac{W_0 W_2 l}{2N\pi^2} \left[ 2(N-1) \sum_a \Gamma_a^i \Gamma_a^j + \sum_{a<b} \Gamma_{ab}^i \Gamma_{ab}^j \right]. \tag{3.14}
\end{aligned}$$

This corrects the vector and tensor disorder terms, and the corresponding counterterms are given by:  $\delta\lambda_1 = \frac{2(N-1)}{N} \lambda_0 \lambda_2 l$  and  $\delta\lambda_2 = \frac{1}{N} \lambda_0 \lambda_2 l$ .

$$\begin{aligned}
\frac{\Pi_{12}^{\text{BCS}}}{(2m)^2} + \frac{\Pi_{12}^{\text{ZS}'}}{(2m)^2} &= 4W_1 W_2 \int \frac{d^d k}{(2\pi)^d} \sum_{a<b,c} \frac{[\Gamma_{ab}^i(\hat{\mathbf{d}}_{\mathbf{k}} \cdot \mathbf{\Gamma}^i) \Gamma_c^i] [\Gamma_{ab}^j(\hat{\mathbf{d}}_{\mathbf{k}} \cdot \mathbf{\Gamma}^j) \Gamma_c^j + \Gamma_c^j(\hat{\mathbf{d}}_{\mathbf{k}} \cdot \mathbf{\Gamma}^j) \Gamma_{ab}^j]}{k^4} \\
&= \frac{W_1 W_2}{4N\pi^2} \ln\left(\frac{\Lambda_{UV}}{\Lambda_{IR}}\right) \sum_{a \neq b, c, f} \Gamma_{ab}^i \Gamma_f^i \Gamma_c^i (\Gamma_c^j \Gamma_f^j \Gamma_{ab}^j + \Gamma_{ab}^j \Gamma_f^j \Gamma_c^j) \\
&= -\frac{W_1 W_2 l}{2N\pi^2} \left[ 2N(N-1) + 3(N-1) \sum_a \Gamma_a^i \Gamma_a^j + \sum_{a<b} \frac{9\Gamma_{ab}^i \Gamma_{ab}^j}{2} \right], \tag{3.15}
\end{aligned}$$

where we have used Eq. (A7). This corrects all the three disorder terms (scalar, vector and tensor), and the corresponding counterterms are given by:  $\delta\lambda_0 = 2(N-1) \lambda_1 \lambda_2 l$ ,  $\delta\lambda_1 = \frac{3(N-1)}{N} \lambda_1 \lambda_2 l$  and  $\delta\lambda_2 = \frac{9}{2N} \lambda_1 \lambda_2 l$ .

### 5. RG equations

The tree-level scaling dimension of the disorder term is  $(2z-d) = \varepsilon + \lambda_0 + N\lambda_1 + \frac{N(N-1)\lambda_2}{2}$ , where  $\varepsilon = 4-d$ . Using Tables I and II, the RG equations for the disorder couplings are thus given

| Coupling    | $\lambda_0$                                   | $\lambda_1$                                      | $\lambda_2$  | $u$ |
|-------------|---|--|--|-----|
| $\lambda_0$ | $\delta\lambda_1 = \frac{1}{N} \lambda_0^2 l$ | $\delta\lambda_0 = 2 \lambda_0 \lambda_1 l$      | $\delta\lambda_1 = \frac{2(N-1)}{N} \lambda_0 \lambda_2 l,$<br>$\delta\lambda_2 = \frac{1}{N} \lambda_0 \lambda_2 l$   | 0   |
| $\lambda_1$ | included in $(\lambda_0, \lambda_1)$ cell     | $\delta\lambda_1 = \frac{3N-2}{N} \lambda_1^2 l$ | $\delta\lambda_0 = 2(N-1) \lambda_1 \lambda_2 l,$<br>$\delta\lambda_1 = \frac{3(N-1)}{N} \lambda_1 \lambda_2 l,$<br>$\delta\lambda_2 = \frac{9}{2N} \lambda_1 \lambda_2 l$ | 0   |
| $\lambda_2$ | included in $(\lambda_0, \lambda_2)$ cell     | included in $(\lambda_1, \lambda_2)$ cell        | $\delta\lambda_0 = \frac{(N-1)!}{4} \lambda_2^2 l$   | 0   |
| $u$         | 0   | 0  | 0  | 0   |

TABLE II. Sum of contributions to the  $\beta$ -functions from the BCS and ZS' diagrams without the  $\frac{k^2}{2m'}$  term, using the same conventions as Table I.

| Coupling    | $\lambda_0$ | $\lambda_1$ | $\lambda_2$ | $u$                                   |
|-------------|-------------|-------------|-------------|---------------------------------------|
| $\lambda_0$ | 0           | 0           | 0           | $\delta\lambda_0 = -4N_f \lambda_0 u$ |
| $\lambda_1$ | 0           | 0           | 0           | 0                                     |
| $\lambda_2$ | 0           | 0           | 0           | 0                                     |
| $u$         | 0           | 0           | 0           | $\delta u = -2N_f u^2$                |

TABLE III. Contributions to the  $\beta$ -functions from the ZS diagram, with the same notation as in Tables I and II. The results are valid for the cases with and without the  $\frac{k^2}{2m'}$  term.

by:

$$\frac{d\lambda_0}{dl} = \left[ \varepsilon + 2\lambda_0 + 2(N+1)\lambda_1 + N(N-1)\lambda_2 \right] \lambda_0 + 2(N-1)\lambda_1\lambda_2 + \frac{(N-1)!}{2} \lambda_2^2, \quad (3.16)$$

$$\frac{d\lambda_1}{dl} = \left[ \varepsilon + \frac{2\lambda_0 + (2N^2 - N + 2)\lambda_1 + (3N^2 - 4N + 1)\lambda_2}{N} \right] \lambda_1 + \frac{\lambda_0 + 2(N-1)\lambda_2}{N} \lambda_0, \quad (3.17)$$

$$\frac{d\lambda_2}{dl} = \left[ \varepsilon + \frac{(2N-3)\lambda_0}{N} + \frac{(4N^2 - 16N + 41)\lambda_1}{2N} \right] \lambda_2 + \frac{(N^3 - 7N^2 + 24N - 24)\lambda_2^2}{N}. \quad (3.18)$$

## B. Addition of the $W_2$ vertex in the presence of Coulomb interactions

### 1. ZS diagram

The ZS diagram with one Coulomb line and one  $W_2$  line attached vanishes upon tracing over spinor indices.

## 2. VC diagrams

The Coulomb correction to the  $W_2$  vertex takes the form:

$$\begin{aligned}
\Gamma_{2c}^{\text{VC}} &= -\frac{2W_2 e^2 \Gamma_{ab}^i}{c} \int \frac{d\omega d^d p}{(2\pi)^{d+1}} \frac{[i\omega + (\mathbf{d}_k \cdot \mathbf{\Gamma}^j)] \Gamma_{ab}^j [i\omega + (\mathbf{d}_k \cdot \mathbf{\Gamma}^j)]}{p^2 (\omega^2 + \mathbf{d}_k^2)^2} \\
&= -\frac{2W_2 e^2 \Gamma_{ab}^i}{c} \times 2\pi^2 \int \frac{d\omega dp p^3}{(2\pi)^{d+1}} \frac{-\omega^2 \Gamma_{ab}^j + \frac{p^4}{2m^2 N} \Gamma_f^j \Gamma_{ab}^j \Gamma_f^j}{p^2 \left(\omega^2 + \frac{p^4}{4m^2}\right)^2} \\
&= \frac{2\pi W_2 e^2 \Gamma_{ab}^i}{c} \int \frac{d\omega dp p^3}{(2\pi)^d} \frac{(\omega^2 - \frac{(N-4)p^4}{4m^2 N})}{p^2 \left(\omega^2 + \frac{p^4}{4m^2}\right)^2} \Gamma_{ab}^j \\
&= \frac{W_2 e^2 \Gamma_{ab}^i \Gamma_{ab}^j}{2\pi^2 c} \int \frac{dp m}{N p} \\
&= \frac{W_2 m e^2 \Gamma_{ab}^i \Gamma_{ab}^j}{2\pi^2 c N} \ln \left( \frac{\Lambda_{UV}}{\Lambda_{IR}} \right) = -\frac{W_2 m e^2 \Gamma_{ab}^i \Gamma_{ab}^j l}{2\pi^2 c N}. \tag{3.19}
\end{aligned}$$

Here we have used Eqs. (2.7) and (A4). The above gives a counterterm  $d\lambda_2 = \frac{4\lambda_2 u l}{N}$ .

The tensor disorder correction to the Coulomb vertex is given by:

$$\Gamma_{c2}^{\text{VC}} = -\frac{e^2}{2c q^2 W_0} \times \Gamma_{02}^{\text{VC}} = -\frac{m^2 e^2 W_2 N(N-1)l}{2c q^2 \pi^2}, \tag{3.20}$$

using Eq. (3.8). This gives the counterterm as  $\delta u = \frac{m^2 W_2 u N(N-1)l}{\pi^2} = \frac{\lambda_2 u N(N-1)l}{2}$ , where an additional minus sign has to be taken into account.

## 3. BCS and ZS' diagrams

These make a vanishing contribution, for reasons discussed in Ref. [8].

## C. RG equations

In the presence of Coulomb interactions, the dynamical critical exponent is given by:

$$z = 2 + \frac{\lambda_0 + N\lambda_1 + \frac{N(N-1)\lambda_2}{2}}{2} - \frac{8u}{15}, \tag{3.21}$$

where  $u = \frac{m e^2}{8\pi^2 c}$ .

Using Tables I, II and III, the full set of the RG equations for the disorder couplings as well as

$u$  is given by:

$$\frac{d\lambda_0}{dl} = \left[ \varepsilon + 2\lambda_0 + 2(N+1)\lambda_1 + N(N-1)\lambda_2 - \frac{(60N_f + 16)u}{15} \right] \lambda_0 + 2(N-1)\lambda_1\lambda_2 + \frac{(N-1)!}{2}\lambda_2^2, \quad (3.22)$$

$$\begin{aligned} \frac{d\lambda_1}{dl} = & \left[ \varepsilon + 2u \left( \frac{N-1}{N} - \frac{8}{15} \right) + \frac{2\lambda_0 + (2N^2 - N + 2)\lambda_1 + (3N^2 - 4N + 1)\lambda_2}{N} \right] \lambda_1 \\ & + \frac{\lambda_0 + 2(N-1)\lambda_2}{N} \lambda_0, \end{aligned} \quad (3.23)$$

$$\frac{d\lambda_2}{dl} = \left[ \varepsilon - \frac{16u}{15} + \frac{4u + (2N-3)\lambda_0}{N} + \frac{(4N^2 - 16N + 41)\lambda_1}{2N} \right] \lambda_2 + \frac{(N^3 - 7N^2 + 24N - 24)\lambda_2^2}{N}, \quad (3.24)$$

$$\frac{du}{dl} = \left[ \varepsilon + 3 \times \frac{\lambda_0 + N\lambda_1 + \frac{N(N-1)\lambda_2}{2}}{2} - \frac{8u}{15} - 2N_f u \right] u. \quad (3.25)$$

Let us examine these equations. First, note that  $\lambda_2 = 0$  is a fixed point - if the action has time-reversal symmetry, the RG flow does not break it. Thus the flow from [8] is contained in the  $\lambda_2 = 0$  subspace of the above equations. Note also that Eqs. (3.24) and (3.25) are sign non-changing, *i.e.* the  $\beta$  function is proportional to the variable itself. As a result, if  $\lambda_2$  and  $u$  start out positive, they must remain non-negative. We will take non-negativity of  $\lambda_2$  and  $u$  for granted in the following discussion. Moreover, for  $\lambda_2 = 0$  the flow reduces to that analyzed in Ref. [8]. Since we are interested in searching for new physics, we assume *positivity* of  $\lambda_2$ .

Now conditioned on positive  $\lambda_2$ , we can see by inspection that  $\lambda_1$  cannot change sign as long as  $\lambda_0$  is non-negative, whereas  $\lambda_0$  cannot change sign as long as  $\lambda_1$  is non-negative. Thus, if  $\lambda_0$  and  $\lambda_1$  start out positive, they can never become negative. Additionally, note that if either  $\lambda_0$  or  $\lambda_1$  (or both) start out zero, then they will be driven positive by  $\lambda_2$ . We thus conclude that we may restrict our attention to regions of positive  $\lambda_0$ ,  $\lambda_1$  and  $\lambda_2$ , and non-negative  $u$ .

Finally, note that for  $N = 5$ , and conditioned on the positivity of the  $\lambda_\alpha$ 's and non-negativity of  $u$ , the  $\beta$  function for  $\lambda_1$  is *strictly positive*. This  $\lambda_1$  must undergo a runaway flow to strong disorder. As such, there is no new fixed point at finite disorder emerging as a result of introducing  $\lambda_2$ , and the result, as in Ref. [8], is a runaway flow to strong disorder.

#### D. Strong-coupling trajectories

From Eq. (3.23), we find that  $\lambda_1$  has a strictly positive  $\beta$  function, *i.e.*, it is monotonically increasing under the RG flow. Therefore, we may view this as an RG time [12] such that we

reparametrize the flows of  $\lambda_{\alpha \neq 1}$  and  $u$  in terms of  $\lambda_1$ . This gives us:

$$\frac{d\lambda_0}{d\lambda_1} = \left[ \varepsilon + 2\lambda_0 + 2(N+1)\lambda_1 + N(N-1)\lambda_2 - \frac{(60N_f + 16)u}{15} \right] \frac{\lambda_0}{\frac{d\lambda_1}{dt}} + \frac{2(N-1)\lambda_1\lambda_2}{\frac{d\lambda_1}{dt}} + \frac{(N-1)!\lambda_2^2}{2\frac{d\lambda_1}{dt}}, \quad (3.26)$$

$$\frac{d\lambda_2}{d\lambda_1} = \left[ \varepsilon - \frac{16u}{15} + \frac{4u + (2N-3)\lambda_0}{N} + \frac{(4N^2 - 16N + 41)\lambda_1}{2N} \right] \frac{\lambda_2}{\frac{d\lambda_1}{dt}} + \frac{(N^3 - 7N^2 + 24N - 24)\lambda_2^2}{N\frac{d\lambda_1}{dt}}, \quad (3.27)$$

$$\frac{du}{d\lambda_1} = \left[ \varepsilon + 3 \times \frac{\lambda_0 + N\lambda_1 + \frac{N(N-1)\lambda_2}{2}}{2} - \frac{8u}{15} - 2N_f u \right] \frac{u}{\frac{d\lambda_1}{dt}}, \quad (3.28)$$

where  $\frac{d\lambda_1}{dt}$  is obtained from Eq. (3.23).

Observing that  $\frac{\varepsilon}{\lambda_1} \rightarrow 0$  under the RG flow, in the trajectories towards strong coupling this ‘tree level’ term is eventually unimportant, and we can simply look at the flow of ratios of couplings, viz.  $\tilde{\lambda}_0 = \frac{\lambda_0}{\lambda_1}$ ,  $\tilde{\lambda}_2 = \frac{\lambda_2}{\lambda_1}$  and  $\tilde{u} = \frac{\lambda_2}{\lambda_1}$ . The flows are then dictated by:

$$\frac{d\tilde{\lambda}_0}{d \ln \lambda_1} \approx -\tilde{\lambda}_0 + \left[ 2\lambda_0 + 2(N+1) + N(N-1)\tilde{\lambda}_2 - \frac{(60N_f + 16)\tilde{u}}{15} \right] \frac{\tilde{\lambda}_0}{den} + \frac{2(N-1)\tilde{\lambda}_2}{den} + \frac{(N-1)!\tilde{\lambda}_2^2}{2den}, \quad (3.29)$$

$$\frac{d\tilde{\lambda}_2}{d \ln \lambda_1} \approx -\tilde{\lambda}_2 + \left[ -\frac{16\tilde{u}}{15} + \frac{4\tilde{u} + (2N-3)\tilde{\lambda}_0}{N} + \frac{(4N^2 - 16N + 41)}{2N} \right] \frac{\tilde{\lambda}_2}{den} + \frac{(N^3 - 7N^2 + 24N - 24)\tilde{\lambda}_2^2}{Nden}, \quad (3.30)$$

$$\frac{d\tilde{u}}{d \ln \lambda_1} \approx -\tilde{u} + \left[ 3 \times \frac{\tilde{\lambda}_0 + N + \frac{N(N-1)\lambda_2}{2}}{2} - \frac{8\tilde{u}}{15} - 2N_f \tilde{u} \right] \frac{\tilde{u}}{den}, \quad (3.31)$$

where

$$den = 2\tilde{u} \left( \frac{N-1}{N} - \frac{8}{15} \right) + \frac{2\tilde{\lambda}_0 + (2N^2 - N + 2) + (3N^2 - 4N + 1)\tilde{\lambda}_2}{N} + \frac{\tilde{\lambda}_0 + 2(N-1)\tilde{\lambda}_2}{N} \tilde{\lambda}_0, \quad (3.32)$$

and we have set  $\frac{\varepsilon}{\lambda_1}$  to zero.

For  $\tilde{\lambda}_2 = 0$  these reduce to the flow equations from [8]. In that work two fixed points  $(\tilde{\lambda}_0, \tilde{\lambda}_2 = 0, \tilde{u})$  were identified: the vector disorder only fixed point  $(0, 0, 0)$ , and the ‘scalar disorder dominated fixed point’  $(9.38516, 0, 0)$ . The former was unstable while the latter one was stable when the flow was restricted to the subspace of  $\lambda_2 = 0$ .

What about non-zero  $\lambda_2$ ? We have verified that there is no new fixed point at non-zero  $\lambda_2$  for any integer  $N_f \geq 1$  i.e. the only fixed points are in the  $\lambda_2 = 0$  subspace

$$\mathcal{F}_1 = (9.38516, 0, 0), \quad \mathcal{F}_2 = (0, 0, 0), \quad (3.33)$$

corresponding to  $(\tilde{\lambda}_0^*, \tilde{\lambda}_2^*, \tilde{u}^*)$ . The linearized flow equations in the vicinity of a fixed point, for  $N_f = 2$ , are given by:

$$\frac{d}{d \ln \lambda_1} \begin{pmatrix} \delta \tilde{\lambda}_0 \\ \delta \tilde{\lambda}_2 \\ \delta \tilde{u} \end{pmatrix} \Big|_{(\tilde{\lambda}_0^*, \tilde{\lambda}_2^*, \tilde{u}^*)} \approx M \begin{pmatrix} \delta \tilde{\lambda}_0 \\ \delta \tilde{\lambda}_2 \\ \delta \tilde{u} \end{pmatrix}, \quad (3.34)$$

where

$$M = \begin{cases} \begin{pmatrix} -0.657005 & -1.63601 & -2.92807 \\ 0 & -0.374747 & 0 \\ 0 & 0 & -0.29875 \end{pmatrix} & \text{for } \mathcal{F}_1, \\ \begin{pmatrix} 0.276596 & 0.851064 & -1.03697 \\ 0 & -0.351064 & 0 \\ 0 & 0 & 0.329787 \end{pmatrix} & \text{for } \mathcal{F}_2. \end{cases} \quad (3.35)$$

The eigenvalues of  $M$  for these three fixed points are given by:

$$(-0.657005, -0.374747, -0.298748) \text{ and } (-0.351064, 0.329787, 0.276596) \quad (3.36)$$

respectively, which shows that  $\mathcal{F}_1$  is stable. Another way to see this is to simply linearize the flow equation for  $\tilde{\lambda}_2$  about the fixed points in the  $\tilde{\lambda}_2 = 0$  subspace - it is straightforward to verify that  $\tilde{\lambda}_2$  is an *irrelevant* perturbation, and so the flow to strong coupling is still controlled by the fixed trajectory  $\mathcal{F}$ , along which tensor disorder and Coulomb interactions vanish.

We therefore conclude that time-reversal symmetry breaking ‘tensor’ disorder is *irrelevant* in the sense that although it grows under renormalization group, its growth is asymptotically slower than the growth of time-reversal preserving scalar and vector disorder, such that the ratio of time-reversal breaking disorder strength to time-reversal preserving disorder strength flows to zero as the problem flows to strong disorder. This is the first main result of our work, and leads us to conjecture that the strong disorder physics should be dominated by time-reversal symmetry preserving disorder. Of course a rigorous treatment of the strong disorder physics is beyond the scope of a perturbative treatment in weak disorder as is employed in this work.

#### IV. PARTICLE-HOLE SYMMETRY BREAKING IN THE BANDSTRUCTURE

Thus far we have assumed that the low energy *bandstructure* is both PH-symmetric and isotropic. In this section we relax the assumption of PH symmetry of the bandstructure (while continuing to

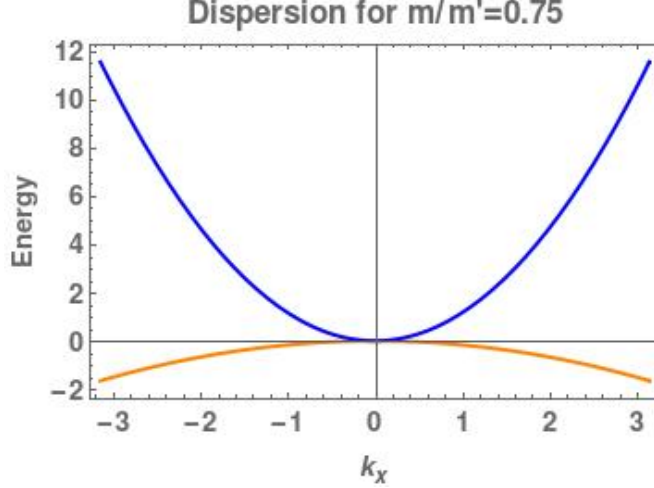


FIG. 3. Quadratic band touching with  $m/m' = 0.75$ .

assume isotropicity). Specifically, we incorporate a scalar  $\frac{k^2}{2m'}$  term in the bandstructure Hamiltonian, such that the bare Green's function becomes

$$G_0(\omega, \mathbf{k}) = \frac{i\omega - \frac{k^2}{2m'} + \mathbf{d}(\mathbf{k}) \cdot \mathbf{\Gamma}}{-\left(i\omega - \frac{k^2}{2m'}\right)^2 + |\mathbf{d}(\mathbf{k})|^2}. \quad (4.1)$$

A finite  $m'$  breaks the PH symmetry of the bare Green's function. Now the two bands touching quadratically have different 'curvatures' as shown in Fig. 3. Note that we require  $m' > m$  in order to be describing a quadratic band touching problem. For  $m' < m$  both bands 'curve' the same way, and for  $m' = m$  one of the bands becomes perfectly flat, and neither of these cases is of interest to us here. Such a PH symmetry-breaking term was shown to be irrelevant in the clean system [1]. However, we aim here to reassess its importance in the presence of disorder.

### A. Renormalization of the particle-hole symmetry-breaking term

In the clean system, the self-energy coming from the Coulomb interaction takes the form:

$$\begin{aligned} \Sigma(\omega, \mathbf{k}) &= -\frac{e^2}{c} \int_{-\infty}^{\infty} \frac{d\Omega}{2\pi} \int \frac{d^d q}{(2\pi)^d} \frac{i\omega + i\Omega - \frac{(\mathbf{k}+\mathbf{q})^2}{2m'} + \mathbf{d}(\mathbf{k}+\mathbf{q}) \cdot \mathbf{\Gamma}}{\left(i\omega + i\Omega - \frac{(\mathbf{k}+\mathbf{q})^2}{2m'}\right)^2 + |\mathbf{d}(\mathbf{k}+\mathbf{q})|^2} V(q) \\ &= -\frac{e^2}{c} \int_{-\infty}^{\infty} \frac{d\Omega}{2\pi} \int \frac{d^d q}{(2\pi)^d} \frac{i\Omega + \mathbf{d}(\mathbf{k}+\mathbf{q}) \cdot \mathbf{\Gamma}}{\Omega^2 + |\mathbf{d}(\mathbf{k}+\mathbf{q})|^2} V(q), \end{aligned} \quad (4.2)$$

where by shifting the integration variable  $\Omega$ , we find that it gives the same correction of  $\left[-\frac{m e^2 \mathbf{d}(\mathbf{k}) \cdot \mathbf{\Gamma}}{15 \pi^2 c} \ln\left(\frac{\Lambda_{UV}}{\Lambda_{IR}}\right)\right]$  as in the PH-symmetric case. Hence, the one-loop renormalized Green's

function becomes

$$G^{-1} = -i\omega + \frac{k^2}{2m'} + \mathbf{d}(\mathbf{k}) \cdot \boldsymbol{\Gamma} \left( 1 + \frac{m e^2}{15\pi^2 c} l \right) = -i\omega + \frac{k^2}{2m'} + \frac{\tilde{\mathbf{d}}(\mathbf{k}) \cdot \boldsymbol{\Gamma}}{m \left( 1 - \frac{8u}{15} l \right)}. \quad (4.3)$$

The requirement of Eq. (2.8) gives  $z = 2 - \frac{8u}{15}$ . Since  $[m'] = 2 - z$ , we find that  $[m']$  has thus changed from 0 at tree-level to  $\frac{8u}{15}$  at one-loop level i.e. it becomes irrelevant, as anticipated in [1]. If we define the ratio  $r_m = \frac{m}{m'}$  to parametrize the strength of PH symmetry-breaking in the bandstructure ( $r_m = 0$  when PH symmetry is exact), then we conclude that that  $[r_m] = -[m'] = z - 2 < 0$  in the clean system, i.e.  $r_m$  flows to zero under RG.

Does disorder change this result? The self-energy contribution from the disorder terms is given by:

$$\begin{aligned} \Sigma(\omega, \mathbf{k}) &= 2W_0 \int \frac{d^d p}{(2\pi)^d} G(\omega, \mathbf{p}) + 2W_1 \int \frac{d^d p}{(2\pi)^d} \Gamma_a G(\omega, \mathbf{p}) \Gamma_a + 2W_2 \int \frac{d^d p}{(2\pi)^d} \Gamma_{ab} G(\omega, \mathbf{k}) \Gamma_{ab} \\ &= \left[ W_0 + N W_1 + \frac{N(N-1)W_2}{2} \right] \left[ \frac{m^2 m' \Lambda_{UV}^2}{4(m^2 - m'^2)\pi^2} + \frac{i\omega m^2 m'^2 (m^2 + m'^2)}{\pi^2 (m^2 - m'^2)^2} \ln \left( \frac{\Lambda_{UV}}{\Lambda_{IR}} \right) \right]. \end{aligned} \quad (4.4)$$

The first term does not have any  $\omega$  or  $\mathbf{k}$  dependence and hence is just a chemical potential renormalization, which should be ignored assuming we have the necessary counterterm to keep the system at the band-crossing point. Invariance of  $[m]$  under the RG thus yields a dynamical exponent

$$z = 2 + \frac{m^2 m'^2 (m^2 + m'^2)}{\pi^2 (m^2 - m'^2)^2} \left[ W_0 + N W_1 + \frac{N(N-1)W_2}{2} \right] = 2 + \frac{m'^2 (m^2 + m'^2)}{2(m^2 - m'^2)^2} \left[ \lambda_0 + N\lambda_1 + \frac{N(N-1)\lambda_2}{2} \right]. \quad (4.5)$$

Now we have  $z > 2$ , such that the PH symmetry-breaking term becomes *relevant* under RG, in sharp contrast to the clean interacting case.

What happens with both disorder and interactions? In this case we have

$$z = 2 + \frac{(1 + r_m^2) \left[ \lambda_0 + N\lambda_1 + \frac{N(N-1)\lambda_2}{2} \right]}{2(1 - r_m^2)^2} - \frac{8u}{15}. \quad (4.6)$$

and  $[r_m] = -[m'] = z - 2$ , where recall  $r_m = m/m'$  is zero for PH-symmetric bandstructures. Now note that the interaction tries to make the PH symmetry-breaking irrelevant, but disorder makes it relevant - and recall also that disorder grows asymptotically more rapidly than interaction under the RG. We therefore conclude that as the problem flows to strong disorder, the strength of PH symmetry-breaking in the bandstructure  $r_m$  must grow. Eventually, there arises a scale where  $r_m(l) = 1$ . At this scale, one of the bands becomes *flat*, there arises a singularity in the density of states, and the whole RG scheme breaks down. We cannot push the RG beyond

$r_m = 1$ . Nevertheless, the prediction that PH symmetry-breaking should be *relevant* in the presence of disorder (whereas it was irrelevant in the clean system) is a non-trivial (and experimentally measurable) prediction of the RG.

## B. Recomputing $\beta$ functions with particle-hole-asymmetric bandstructure

In this section we recompute the  $\beta$  functions with PH-asymmetric band-structures, still assuming  $m' > m$  i.e.  $r_m < 1$ . This requires a re-evaluation of the integrals for all the constituent diagrams (but not a re-evaluation of combinatorial pre-factors or signs).

### 1. Clean system

We begin with the clean system. For the diagram emerging from the contractions of the product of two Coulomb terms with the ZS topology, we obtain the contribution

$$\Pi_{\text{cc}}^{\text{ZS}}(\mathbf{q}) = -\frac{2N_f}{q^4} \left(\frac{e^2}{2c}\right)^2 \text{Tr} \left[ \int \frac{d^d k d\omega}{(2\pi)^{d+1}} \frac{\left\{ i\omega - \frac{(\mathbf{k}+\mathbf{q})^2}{2m'} + \mathbf{d}(\mathbf{k}+\mathbf{q}) \cdot \boldsymbol{\Gamma} \right\} \left\{ i\omega - \frac{k^2}{2m'} + \mathbf{d}(\mathbf{k}) \cdot \boldsymbol{\Gamma} \right\}}{\left\{ -\left( i\omega - \frac{(\mathbf{k}+\mathbf{q})^2}{2m'} \right)^2 + |\mathbf{d}(\mathbf{k}+\mathbf{q})|^2 \right\} \left\{ -\left( i\omega - \frac{k^2}{2m'} \right)^2 + |\mathbf{d}(\mathbf{k})|^2 \right\}} \right].$$

We choose  $\mathbf{q}$  to lie along the  $z$  axis, without any loss of generality. Dropping the terms that will vanish upon performing the angular integrals, and performing the  $\omega$  integral by the method of residues, we get

$$\Pi_{\text{cc}}^{\text{ZS}}(\mathbf{q}) = -\frac{8N_f m'^2 e^2}{c^2 q^4} \int \frac{d^d k}{(2\pi)^d} \frac{|\mathbf{d}(\mathbf{k}+\mathbf{q})| + |\mathbf{d}(\mathbf{k})|}{4(|\mathbf{d}(\mathbf{k}+\mathbf{q})| + |\mathbf{d}(\mathbf{k})|)^2 m'^2 + (q^2 + 2kq \cos \theta)^2} \left( \frac{\mathbf{d}(\mathbf{k}+\mathbf{q}) \cdot \mathbf{d}(\mathbf{k})}{|\mathbf{d}(\mathbf{k}+\mathbf{q})||\mathbf{d}(\mathbf{k})|} - 1 \right). \quad (4.7)$$

Since the above integral manifestly vanishes for  $\mathbf{q} = 0$ , we can obtain the divergent part from the leading order term in  $q$  after Taylor expanding in small  $q$ , as follows:

$$\Pi_{\text{cc}}^{\text{ZS}}(\mathbf{q}) = \frac{8N_f e^2}{c^2 q^4} \int \frac{d^d k}{(2\pi)^d} \frac{3m q^2}{4k^4} \sin^2 \theta, \quad (4.8)$$

This has the same form as in the PH-symmetric case and gives the same correction of  $\frac{e^2}{2c} \rightarrow \frac{e^2}{2c} \left[ 1 - \frac{m e^2}{4\pi^2 c} N_f l \right]$ . As shown in Appendix B, the remaining diagrams (VC, ZS', BCS) do not have any divergent contribution and thus the PH symmetry-breaking term does not affect the RG flows of the clean system.

## 2. Disordered non-interacting system

A VC diagram with two scalar ( $W_0$ ) lines can emerge in 8 distinct ways; including factors from (3.3) we find a correction to the scalar vertex from

$$\begin{aligned}
\Gamma_{00}^{\text{VC}} &= 4 W_0^2 \int \frac{d^d k}{(2\pi)^d} \frac{\left[ \left( i\omega - \frac{k^2}{2m'^2} \right) + \mathbf{d}_k \cdot \mathbf{\Gamma}^j \right] \left[ \left( i\omega - \frac{k^2}{2m'^2} \right) + \mathbf{d}_k \cdot \mathbf{\Gamma}^j \right]}{\left[ - \left( i\omega - \frac{k^2}{2m'^2} \right)^2 + \frac{k^4}{4m^2} \right]^2} \\
&= 4 W_0^2 \int \frac{d^d k}{(2\pi)^d} \frac{\left( i\omega - \frac{k^2}{2m'^2} \right)^2 + \frac{k^4}{4m^2}}{\left[ - \left( i\omega - \frac{k^2}{2m'^2} \right)^2 + \frac{k^4}{4m^2} \right]^2} \\
&= \frac{2 W_0^2}{\pi^2} \frac{m^2 m'^2 (m^2 + m'^2)}{(m^2 - m'^2)^2} \ln \left( \frac{\Lambda_{\text{UV}}}{\Lambda_{\text{IR}}} \right). \tag{4.9}
\end{aligned}$$

For the rest of the non-vanishing VC, BCS and ZS' diagrams we have to use the integral:

$$I = \int \frac{d^d k}{(2\pi)^d} \frac{\frac{k^4}{4m^2}}{\left( -\frac{k^4}{4m^2} + \frac{k^4}{4m^2} \right)^2} = \frac{m^2 m'^4}{2\pi^2 (m^2 - m'^2)^2} \ln \left( \frac{\Lambda_{\text{UV}}}{\Lambda_{\text{IR}}} \right), \tag{4.10}$$

which appears as a prefactor for each. This can be implemented by replacing  $m^2 \rightarrow m^2 \mu$ , where  $\mu \equiv \frac{m'^4}{(m^2 - m'^2)^2} = \frac{1}{(1 - r_n^2)^2}$ , in the answers obtained for the PH-symmetric case.

## 3. Disordered interacting problem

We now consider diagrams with mixed interaction and disorder lines. We start with the ZS diagram with one scalar disorder and one Coulomb line (all other ZS diagrams vanish upon taking the trace). We have

$$\Pi_{c0}^{\text{ZS}} = -2 W_0 \times \frac{2 c q^2}{e^2} \Pi_{cc}^{\text{ZS}} = -\frac{N_f m e^2 W_0}{2\pi^2 c} \ln \left( \frac{\Lambda_{\text{UV}}}{\Lambda_{\text{IR}}} \right), \tag{4.11}$$

which is same as the PH-symmetric case.

We now consider vertex corrections. The Coulomb correction to a  $W_0$  disorder vertex vanishes ( $\Gamma_{0c}^{\text{VC}} = 0$ ) as before. The Coulomb correction to the  $W_1$  vertex takes the form:

$$\begin{aligned}
\Gamma_{1c}^{\text{VC}} &= -\frac{4 W_1 e^2}{2 c} \Gamma_a^i \int \frac{d\omega}{2\pi} \frac{d^d p}{(2\pi)^d} G(\omega, \mathbf{p}) \Gamma_a^j G(\omega, \mathbf{p}) \\
&= \frac{2 e^2 W_1}{c} \Gamma_a^i \Gamma_a^j \int \frac{d\omega}{2\pi} \frac{d^d p}{(2\pi)^d} \frac{- \left( i\omega - \frac{p^2}{2m'^2} \right)^2 + \frac{N-2}{N} \frac{p^4}{4m^2}}{p^2 \left[ - \left( i\omega - \frac{p^2}{2m'^2} \right)^2 + \frac{p^4}{4m^2} \right]^2} \\
&= \frac{2 e^2 W_1}{c} \Gamma_a^i \Gamma_a^j \int \frac{d\omega}{2\pi} \frac{d^d p}{(2\pi)^d} \frac{\omega^2 + \frac{N-2}{N} \frac{p^4}{4m^2}}{p^2 \left[ \omega^2 + \frac{p^4}{4m^2} \right]^2}, \tag{4.12}
\end{aligned}$$

| Coupling    | $\lambda_0$   | $\lambda_1$   | $\lambda_2$   | $u$  |
|-------------|---|---|---|--|
| $\lambda_0$ | $\delta\lambda_0 = (1 + r_m^2) \mu \lambda_0^2 l$           | $\delta\lambda_1 = -\frac{N-2}{N} \mu \lambda_0 \lambda_1 l$    | $\delta\lambda_0 = \frac{N(N-1)}{2} \mu \lambda_0 \lambda_2 l$            | 0  |
| $\lambda_1$ | $\delta\lambda_0 = N \mu \lambda_0 \lambda_1 l$             | $\delta\lambda_1 = \frac{(N-2)^2}{N} \mu \lambda_1^2 l$         | $\delta\lambda_1 = -\frac{(N-1)(N-2)(N-4)}{2N} \mu \lambda_1 \lambda_2 l$ | $\delta\lambda_1 = \frac{2(N-1)}{N} \lambda_1 u l$ |
| $\lambda_2$ | $\delta\lambda_2 = \frac{N-4}{N} \mu \lambda_0 \lambda_2 l$ | $\delta\lambda_2 = \frac{(N-4)^2}{N} \mu \lambda_1 \lambda_2 l$ | $\delta\lambda_2 = \frac{(N-4)(N^2-9N+12)}{2N} \mu \lambda_2^2 l$         | $d\lambda_2 = \frac{4}{N} \lambda_2 u l$           |
| $u$         | $\delta u = \mu \lambda_0 u l$                              | $\delta u = N \mu \lambda_1 u l$                                | $\delta u = \frac{N(N-1)}{2} \mu \lambda_2 u l$                           | 0  |

TABLE IV. Contributions to the  $\beta$ -functions from the VC diagrams with the  $\frac{k^2}{2m'}$  term. Here,  $\lambda_\alpha = \frac{2m^2 W_\alpha}{\pi^2}$ ,  $u = \frac{m e^2}{8\pi^2 c}$ ,  $\mu = \frac{1}{(1-r_m^2)^2}$  and  $l$  is the RG flow parameter.

which is the same expression as in the PH-symmetric case. Similarly, the Coulomb correction to the  $W_2$  vertex also gives the same result as in Eq. 3.19.

Finally, we have:

$$\Gamma_{c0}^{\text{VC}} = -\frac{e^2}{2c q^2 W_0} \times \Gamma_{00}^{\text{VC}} = -\frac{m^2 m'^4}{(m^2 - m'^2)^2} \frac{e^2 W_0}{c q^2 \pi^2} \ln \left( \frac{\Lambda_{\text{UV}}}{\Lambda_{\text{IR}}} \right), \quad (4.13)$$

$$\Gamma_{c1}^{\text{VC}} = -\frac{e^2}{2c q^2 W_0} \times \Gamma_{01}^{\text{VC}} = -\frac{m^2 m'^4}{(m^2 - m'^2)^2} \frac{N e^2 W_1}{c q^2 \pi^2} \ln \left( \frac{\Lambda_{\text{UV}}}{\Lambda_{\text{IR}}} \right), \quad (4.14)$$

and

$$\Gamma_{c2}^{\text{VC}} = -\frac{e^2}{2c q^2 W_0} \times \Gamma_{02}^{\text{VC}} = -\frac{m^2 m'^4}{(m^2 - m'^2)^2} \frac{e^2 W_2 N (N-1)}{2c q^2 \pi^2} \ln \left( \frac{\Lambda_{\text{UV}}}{\Lambda_{\text{IR}}} \right), \quad (4.15)$$

ZS' and BCS diagrams with mixed disorder and interaction lines do not produce logarithmically divergent corrections, for the reasons identified in [8].

### C. RG equations

Firstly, we recall that in the presence of Coulomb interactions and disorder, the dynamical critical exponent is given by:

$$z = 2 + \frac{(1 + r_m^2) \left[ \lambda_0 + N \lambda_1 + \frac{N(N-1)\lambda_2}{2} \right]}{2(1 - r_m^2)^2} - \frac{8u}{15}. \quad (4.16)$$

Using tables IV, V and III, we can write down the full set of the RG equations for the disorder

| Coupling    | $\lambda_0$                                       | $\lambda_1$  | $\lambda_2$  | $u$ |
|-------------|---|--|--|-----|
| $\lambda_0$ | $\delta\lambda_1 = \frac{1}{N} \mu \lambda_0^2 l$ | $\delta\lambda_0 = 2 \mu \lambda_0 \lambda_1 l$      | $\delta\lambda_1 = \frac{2(N-1)}{N} \mu \lambda_0 \lambda_2 l,$<br>$\delta\lambda_2 = \frac{1}{N} \mu \lambda_0 \lambda_2 l$   | 0   |
| $\lambda_1$ | included in $(\lambda_0, \lambda_1)$ cell         | $\delta\lambda_1 = \frac{3N-2}{N} \mu \lambda_1^2 l$ | $\delta\lambda_0 = 2(N-1) \mu \lambda_1 \lambda_2 l,$<br>$\delta\lambda_1 = \frac{3(N-1)}{N} \mu \lambda_1 \lambda_2 l,$<br>$\delta\lambda_2 = \frac{9}{2N} \mu \lambda_1 \lambda_2 l$ | 0   |
| $\lambda_2$ | included in $(\lambda_0, \lambda_2)$ cell         | included in $(\lambda_1, \lambda_2)$ cell            | $\delta\lambda_0 = \frac{(N-1)!}{4} \mu \lambda_2^2 l$   | 0   |
| $u$         | 0   | 0  | 0  | 0   |

TABLE V. Sum of contributions to the  $\beta$ -functions from the BCS and ZS' diagrams with the  $\frac{k^2}{2m'}$  term, using the same conventions as Table IV.

couplings as well as  $u$ , when we include the  $\frac{k^2}{2m'}$  term. We note that

$$\begin{aligned} \frac{d\lambda_0}{dl} = & \left[ \varepsilon + 2(1 + r_m^2) \mu \lambda_0 + (2 + 2N + N r_m^2) \mu \lambda_1 + \frac{N(N-1)(2 + r_m^2) \mu \lambda_2}{2} - \frac{(60N_f + 16)u}{15} \right] \lambda_0 \\ & + \left[ 2(N-1) \lambda_1 + \frac{(N-1)!}{2} \lambda_2 \right] \mu \lambda_2, \end{aligned} \quad (4.17)$$

$$\begin{aligned} \frac{d\lambda_1}{dl} = & \left[ \varepsilon + 2u \left( \frac{N-1}{N} - \frac{8}{15} \right) + \frac{2(2 + N r_m^2) \mu \lambda_0 + (N-1)(r_m^2 N^2 + 6N - 2) \mu \lambda_2}{2N} \right. \\ & \left. + \frac{(2 - N + r_m^2 N^2 + 2N^2) \mu \lambda_1}{N} \right] \lambda_1 + \frac{\lambda_0 + 2(N-1) \lambda_2}{N} \mu \lambda_0, \end{aligned} \quad (4.18)$$

$$\begin{aligned} \frac{d\lambda_2}{dl} = & \left[ \varepsilon - \frac{16u}{15} + \frac{4u + (2N + N r_m^2 - 3) \mu \lambda_0}{N} + \frac{(4N^2 + 2N^2 r_m^2 - 16N + 41) \mu \lambda_1}{2N} \right. \\ & \left. + \frac{N\{48 - 2N(7 - N) + N(N-1)r_m^2\} - 48}{2N} \mu \lambda_2 \right] \lambda_2, \end{aligned} \quad (4.19)$$

$$\frac{du}{dl} = \left[ \varepsilon + (3 + r_m^2) \times \frac{\lambda_0 + N \lambda_1 + \frac{N(N-1)\lambda_2}{2} \mu}{2} - \frac{8u}{15} - 2N_f u \right] u, \quad (4.20)$$

$$\frac{dr_m}{dl} = \left[ \frac{(1 + r_m^2) \left\{ \lambda_0 + N \lambda_1 + \frac{N(N-1)\lambda_2}{2} \right\}}{2(1 - r_m^2)^2} - \frac{8u}{15} \right] r_m. \quad (4.21)$$

These equations reduce the the PH-symmetric equations when we take  $r_m \rightarrow 0$  and  $\mu \rightarrow 1$ .

Now let us discuss the fixed point structure of the above equations. Firstly, note that the  $\beta$  functions for  $\lambda_2$  and  $u$  are proportional to the variables themselves, and so these variables cannot change sign, nor can they be generated ‘from nothing’ under RG. If they start out positive, they must remain positive forever. Next, note that (given the non-negativity of  $\lambda_2$ ), it follows from arguments analogous to those advanced in the PH-symmetric case that  $\lambda_0$  and  $\lambda_1$  cannot become negative, if they start out with non-negative initial values. We thus conclude that all four couplings  $\lambda_{1,2,3}$  and  $u$  must be non-negative.

Now note that for non-negative couplings, with  $N = 5$  and  $0 \leq r_m < 1$ , the beta function

for  $\lambda_1$  is strictly positive, so that  $\lambda_1$  must grow without limit i.e. there is not any finite disorder fixed point of the perturbative RG, even after we allow for PH symmetry breaking. Thus the PH-asymmetric problem also flows to strong disorder.

Finally, a consideration of the equation for  $r_m$  with growing  $\lambda_i, u$  leads to the conclusion that there is no fixed point at  $0 < r_m < 1$ . The only fixed point for this equation is at  $r_m = 0$ , and this fixed point is *unstable* in the presence of disorder (as has been discussed). Thus,  $r_m$  increases without limit under perturbative RG (although the RG scheme itself starts to break down when  $r_m \rightarrow 1$ , at which point one of the two bands becomes flat, and the co-efficient  $\mu$  becomes singular).

#### D. Strong-coupling trajectories

From Eq. (4.18), we find that  $\lambda_1$  has a strictly positive  $\beta$  function, *i.e.*, it is monotonically increasing under the RG flow. Therefore, we may view this as an RG time such that we reparametrize the flows of  $\lambda_{\alpha \neq 1}$ ,  $u$  and  $r_m$  in terms of  $\lambda_1$ . This gives us:

$$\begin{aligned} \frac{d\lambda_0}{d\lambda_1} &= \left[ \varepsilon + 2(1 + r_m^2) \mu \lambda_0 + (2 + 2N + N r_m^2) \mu \lambda_1 + \frac{N(N-1)(2 + r_m^2) \mu \lambda_2}{2} - \frac{(60N_f + 16)u}{15} \right] \frac{\lambda_0}{\frac{d\lambda_1}{dt}} \\ &+ \left[ 2(N-1) \lambda_1 + \frac{(N-1)!}{2} \lambda_2 \right] \frac{\mu \lambda_2}{\frac{d\lambda_1}{dt}}, \end{aligned} \quad (4.22)$$

$$\begin{aligned} \frac{d\lambda_2}{d\lambda_1} &= \left[ \varepsilon - \frac{16u}{15} + \frac{4u + (2N + N r_m^2 - 3) \mu \lambda_0}{N} + \frac{(4N^2 + 2N^2 r_m^2 - 16N + 41) \mu \lambda_1}{2N} \right. \\ &+ \left. \frac{N\{48 - 2N(7 - N) + N(N-1)r_m^2\} - 48}{2N} \mu \lambda_2 \right] \frac{\lambda_2}{\frac{d\lambda_1}{dt}}, \end{aligned} \quad (4.23)$$

$$\frac{du}{d\lambda_1} = \left[ \varepsilon + (3 + r_m^2) \times \frac{\lambda_0 + N \lambda_1 + \frac{N(N-1)\lambda_2}{2}}{2} \mu - \frac{8u}{15} - 2N_f u \right] \frac{u}{\frac{d\lambda_1}{dt}}, \quad (4.24)$$

$$\frac{dr_m}{d\lambda_1} = \left[ \frac{(1 + r_m^2) \left\{ \lambda_0 + N \lambda_1 + \frac{N(N-1)\lambda_2}{2} \right\}}{2(1 - r_m^2)^2} - \frac{8u}{15} \right] \frac{r_m}{\frac{d\lambda_1}{dt}}, \quad (4.25)$$

where  $\frac{d\lambda_1}{dt}$  is obtained from Eq. (4.18).

Observing that  $\frac{\varepsilon}{\lambda_1} \rightarrow 0$  under the RG flow, in the trajectories towards strong coupling this ‘tree level’ term is eventually unimportant, and we can simply look at the flow of ratios of couplings,

viz.  $\tilde{\lambda}_0 = \frac{\lambda_0}{\lambda_1}$ ,  $\tilde{\lambda}_2 = \frac{\lambda_2}{\lambda_1}$  and  $\tilde{u} = \frac{\lambda_2}{\lambda_1}$ . The flows are then dictated by:

$$\begin{aligned} \frac{d\lambda_0}{d\ln\lambda_1} &\approx -\tilde{\lambda}_0 + \left[ 2(N-1) + \frac{(N-1)!}{2} \tilde{\lambda}_2 \right] \frac{\mu \tilde{\lambda}_2}{den'} \\ &\quad + \left[ 2(1+r_m^2) \mu \tilde{\lambda}_0 + (2+2N+N r_m^2) \mu + \frac{N(N-1)(2+r_m^2) \mu \tilde{\lambda}_2}{2} - \frac{(60N_f+16) \tilde{u}}{15} \right] \frac{\tilde{\lambda}_0}{den'}, \end{aligned} \quad (4.26)$$

$$\begin{aligned} \frac{d\lambda_2}{d\ln\lambda_1} &\approx -\tilde{\lambda}_2 + \left[ -\frac{16\tilde{u}}{15} + \frac{4\tilde{u} + (2N+N r_m^2 - 3) \mu \tilde{\lambda}_0}{N} + \frac{(4N^2 + 2N^2 r_m^2 - 16N + 41) \mu}{2N} \right. \\ &\quad \left. + \frac{N\{48 - 2N(7-N) + N(N-1)r_m^2\} - 48}{2N} \mu \tilde{\lambda}_2 \right] \frac{\tilde{\lambda}_2}{den'}, \end{aligned} \quad (4.27)$$

$$\frac{du}{d\ln\lambda_1} \approx -\tilde{u} + \frac{\left[ (3+r_m^2) \times \frac{\lambda_0+N+\frac{N(N-1)\tilde{\lambda}_2}{2}}{2} \mu - \frac{8\tilde{u}}{15} - 2N_f \tilde{u} \right] \tilde{u}}{den'}, \quad (4.28)$$

$$\frac{dr_m}{d\ln\lambda_1} \approx \frac{\left[ \frac{(1+r_m^2) \left\{ \tilde{\lambda}_0+N+\frac{N(N-1)\tilde{\lambda}_2}{2} \right\}}{2(1-r_m^2)^2} - \frac{8\tilde{u}}{15} \right] r_m}{den'}, \quad (4.29)$$

where

$$\begin{aligned} den' &= 2\tilde{u} \left( \frac{N-1}{N} - \frac{8}{15} \right) + \frac{2(2+N r_m^2) \mu \tilde{\lambda}_0 + (N-1)(r_m^2 N^2 + 6N - 2) \mu \tilde{\lambda}_2}{2N} \\ &\quad + \frac{(2-N+r_m^2 N^2 + 2N^2) \mu}{N} + \frac{\tilde{\lambda}_0 + 2(N-1) \tilde{\lambda}_2}{N} \mu \tilde{\lambda}_0, \end{aligned} \quad (4.30)$$

and we have set  $\frac{\epsilon}{\lambda_1}$  to zero.

For any integer  $N_f \geq 1$ , we obtain the following non-negative fixed points:

$$\mathcal{F}'_1 = (9.38516, 0, 0, 0), \quad \mathcal{F}'_2 = (0, 0, 0, 0), \quad (4.31)$$

corresponding to  $(\tilde{\lambda}_0^*, \tilde{\lambda}_2^*, \tilde{u}^*, r_m^*)$ . These are the same fixed points that were obtained in the case with PH symmetry. It follows from our earlier analysis that  $\mathcal{F}'_1$  is stable in the  $(\tilde{\lambda}_0^*, \tilde{\lambda}_2^*, \tilde{u}^*)$  subspace, whereas  $\mathcal{F}'_2$  is unstable. However, both fixed points are unstable in the  $r_m$  direction.

We have also calculated the fixed points in the ratio space as functions of  $r_m$  (treating  $r_m$  as a fixed rather than flowing parameter) in order to illuminate how the relevant PH symmetry-breaking affects the RG flow. The nature of the fixed points are still of the form  $(\tilde{\lambda}_0^*, 0, 0)$ ,  $(0, 0, 0)$ , with a positive  $\tilde{\lambda}_0^*$ . The first fixed point is stable, while the second one is unstable. The behaviour of  $\tilde{\lambda}_0^*$  as a function of  $r_m$  is shown in Fig. 4. This gives us a sense of how the flow in the coupling space changes as PH symmetry-breaking becomes strong. Importantly, while the ratio of scalar to vector disorder changes (so that scalar disorder becomes more important as the PH symmetry-breaking becomes strong), tensor disorder and the long range interaction continue to grow asymptotically more slowly than scalar and vector disorder, and may continue to be ignored in a first approximation.

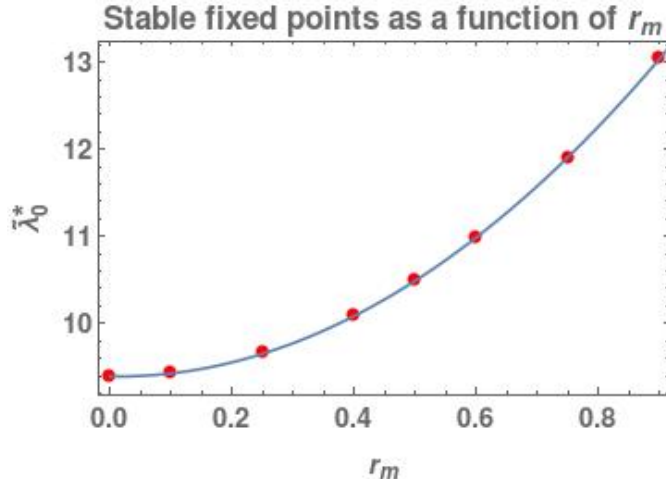


FIG. 4. Behaviour of the scalar-vector disorder ratio as a function of  $r_m$ , at the stable fixed point of the ratio space.

## V. ANALYSIS AND DISCUSSION

We have analyzed the interplay of short-range disorder and Coulomb interactions about quadratic band crossings in three dimensions, using a perturbative renormalization group procedure. Unlike earlier work [7, 8], we have not restricted ourselves to time-reversal symmetry preserving disorder, nor have we assumed that the bandstructure is PH-symmetric. We have shown that the full problem, including all types of disorder as well as PH asymmetry in the bandstructure, does not admit any non-trivial stable fixed points at weak coupling, and exhibits a runaway flow to strong disorder. Along the flow to strong disorder, time-reversal-symmetry-preserving disorder grows asymptotically faster than time-reversal-symmetry-breaking disorder and the Coulomb interaction. Thus, we conjecture that at a first pass, both time-reversal-symmetry-breaking disorder and Coulomb interactions may be neglected in describing the strong-coupling phase, and only time-reversal-preserving disorder needs to be taken into account. In this respect, the general problem that we study herein ‘flows’ into the simpler problem tackled in [8], and the discussion in [8] regarding the strong-coupling phase may be carried over *mutatis mutandis*, and two phases (a diffusive metal and a localized phase) may be predicted. Of course, arguments about the strong-coupling regime based on extrapolation from weak coupling must be treated with caution, and a careful discussion of the strong-coupling physics would require construction of the appropriate sigma model. Furthermore, even if time-reversal-symmetry-breaking disorder is asymptotically weaker than time-reversal-symmetry-preserving disorder, it may still have important effects by changing the symmetry class of the problem. Nevertheless, our results do suggest that in describing the strong-coupling phase, it should be sufficient to *start* with an analysis of the effects of strong time-reversal-symmetry-preserving disorder, and then to incorporate time-

reversal-symmetry-breaking disorder and the Coulomb interaction as perturbations. Construction of such a description of the strong-coupling phase would be an interesting challenge for future work.

Our analysis also reveals that PH symmetry-breaking in the *bandstructure* is *relevant* in the presence of disorder. This is in sharp contrast to the situation that appears in clean systems [1], where such a perturbation is *irrelevant*. In consequence, even if at high energies the conduction and valence bands appear to have similar ‘masses’, the low-energy bandstructure will display strong asymmetry in the effective mass of the two bands (see e.g. Fig. 3). This is a non-trivial prediction of our analysis, which could be directly probed in, for e.g., ARPES experiments, and would provide a *direct* experimental diagnostic of whether disorder physics dominates a particular sample, or whether the sample may be treated as ‘effectively clean’.

**Acknowledgements** R.M.N. would like to thank S.A. Parameswaran for a previous collaboration on a related problem, and Y.Z. Chou for useful discussions. R.M.N.’s research was sponsored by the U.S. Army Research Office and was accomplished under Grant Number W911NF-17-1-0482. The views and conclusions contained in this document are those of the authors and should not be interpreted as representing the official policies, either expressed or implied, of the Army Research Office or the U.S. Government. The U.S. Government is authorized to reproduce and distribute reprints for Government purposes notwithstanding any copyright notation herein.

## Appendix A: Clifford algebra and various identities

In this appendix, we list various identities which follow from the Clifford algebra. First, for  $N$  gamma matrices  $\Gamma_a$  ( $a = 1, 2, \dots, N$ ), we have

$$\sum_a \Gamma_a \Gamma_a = N. \quad (\text{A1})$$

Other relations that have been used in various computations in the main text are:

$$\sum_{a < b} \Gamma_{ab} \Gamma_{ab} = \frac{N(N-1)}{2}, \quad (\text{A2})$$

$$\Gamma_{cd} \Gamma_a = i(\delta_{ac} \Gamma_d - \delta_{ad} \Gamma_c) + \Gamma_a \Gamma_{cd}, \quad (\text{A3})$$

$$\Gamma_{cd} \Gamma_a \Gamma_{cd} = \frac{(N-1)(N-4)}{2} \Gamma_a, \quad (\text{A4})$$

$$\Gamma_f \Gamma_{ab} \Gamma_f = (N-4) \Gamma_{ab}. \quad (\text{A5})$$

Since  $N = 5$  for the current problem, we can use the relation:

$$\Gamma_{ab} \Gamma_f = \Gamma]_f \Gamma_{ab} = i(\delta_{af} \Gamma_b - \delta_{bf} \Gamma_a) - \frac{\varepsilon_{abfcd} \Gamma_{cd}}{2}. \quad (\text{A6})$$

Hence we have:

$$\begin{aligned}
& \sum_{a<b,c,f} \Gamma_{ab}^i \Gamma_f^i \Gamma_c^i (\Gamma_c^j \Gamma_f^j \Gamma_{ab}^j + \Gamma_{ab}^j \Gamma_f^j \Gamma_c^j) \\
&= -2(N-1) \sum_{a,b} \Gamma_a^i \Gamma_b^i (\Gamma_a^j \Gamma_b^j + \Gamma_b^j \Gamma_a^j) + \sum_{a<b,c} \frac{3\Gamma_{ab}^i \Gamma_c^i}{2} (\Gamma_c^j \Gamma_{ab}^j + \Gamma_{ab}^j \Gamma_c^j) \\
&= 4N(N-1) - 6(N-1) \sum_a \Gamma_a^i \Gamma_a^j + \sum_{a<b} \frac{9\Gamma_{ab}^i \Gamma_{ab}^j}{2}. \tag{A7}
\end{aligned}$$

**Appendix B: Vanishing divergent contributions from the VC, BCS, ZS' diagrams in the clean system with  $\frac{k^2}{2m'}$  term.**

For the PH-symmetric clean system, it was shown in Ref. [8] that the VC, BCS, and ZS' diagrams give no divergent contribution. Here we verify that the above statement holds even in the presence of the  $\frac{k^2}{2m'}$  term.

The vertex correction with two Coulomb lines has a relative minus sign compared to ZS and takes the form:

$$\begin{aligned}
\Gamma_{00}^{\text{VC}} &\propto -\frac{e^4}{c^2 q^2} \int d\omega d^d k \frac{G(\omega, \mathbf{p})G(\omega, \mathbf{p} + \mathbf{q})}{k^2} \\
&\propto -\frac{e^4}{c^2 q^2} \int d\omega d^d k \frac{\{i\omega - \frac{(\mathbf{k}+\mathbf{q})^2}{2m'} + \mathbf{d}(\mathbf{k} + \mathbf{q}) \cdot \mathbf{\Gamma}\} \{i\omega - \frac{k^2}{2m'} + \mathbf{d}(\mathbf{k}) \cdot \mathbf{\Gamma}\}}{k^2 \left\{ - \left( i\omega - \frac{(\mathbf{k}+\mathbf{q})^2}{2m'} \right)^2 + |d(\mathbf{k} + \mathbf{q})|^2 \right\} \left\{ - \left( i\omega - \frac{k^2}{2m'} \right)^2 + |d(\mathbf{k})|^2 \right\}}. \tag{B1}
\end{aligned}$$

We choose  $\mathbf{q}$  to lie along the  $z$  axis, without any loss of generality. Dropping the terms that will vanish upon performing the angular integrals, and performing the  $\omega$  integral by the method of residues, we get

$$\Gamma_{00}^{\text{VC}} \propto -\frac{e^4}{c^2 q^2} \int \frac{d^d k}{k^2} \frac{|\mathbf{d}(\mathbf{k} + \mathbf{q})| + |\mathbf{d}(\mathbf{k})|}{4(|\mathbf{d}(\mathbf{k} + \mathbf{q})| + |\mathbf{d}(\mathbf{k})|)^2 m'^2 + (q^2 + 2kq \cos \theta)^2} \left( \frac{\mathbf{d}(\mathbf{k} + \mathbf{q}) \cdot \mathbf{d}(\mathbf{k})}{|\mathbf{d}(\mathbf{k} + \mathbf{q})||\mathbf{d}(\mathbf{k})|} - 1 \right). \tag{B2}$$

Since the above integral manifestly vanishes for  $\mathbf{q} = 0$ , we can obtain the possible divergent part from the leading order term in  $q$  after Taylor expanding in small  $q$ , as follows:

$$\Gamma_{00}^{\text{VC}} \propto -\frac{e^4}{c^2} \int d^d k \frac{3m \sin^2 \theta}{4k^6}, \tag{B3}$$

which diverges as  $1/q^2$  i.e produces a correction to the Coulomb line, but only a constant correction (since there is no log divergence). Thus, this diagram does not contribute the the  $\beta$  functions of the clean system.

The ZS' and BCS diagrams correspond to the ladder and twisted ladder diagram topologies (“Cooperon” and “diffuson”). Denoting the incoming momenta by  $\mathbf{k}_1$  and  $\mathbf{k}_2$ , and the outgoing

momenta by  $\mathbf{k}_1 + \mathbf{q}$  and  $\mathbf{k}_2 - \mathbf{q}$ , we note that for extracting the possible divergent part, although the external momenta  $\mathbf{k}_1$  and  $\mathbf{k}_2$  can be set to zero, the momentum transfer  $\mathbf{q}$  cannot be, as it is needed to split a high order pole in the integrand coming from the doubled Coulomb line [13]. However, we can choose  $\mathbf{q}$  to lie along the  $z$  axis, without any loss of generality. The sum of these two diagrams with two Coulomb lines gives (note the overall minus sign with respect to ZS):

$$\Pi_{00}^{\text{ZS}'} + \Pi_{00}^{\text{BCS}} \propto -e^4 \int \frac{d\omega d^d k}{k^2 |\mathbf{k} - \mathbf{q}|^2} G(\omega, \mathbf{k}) [G(\omega, \mathbf{k} - \mathbf{q}) + G(-\omega, -\mathbf{k})] \quad (\text{B4})$$

$$\begin{aligned} \propto -e^4 \int \frac{d\omega d^d k}{k^2 |\mathbf{k} - \mathbf{q}|^2} & \left[ \frac{\{i\omega - \frac{(\mathbf{k}+\mathbf{q})^2}{2m'} + \mathbf{d}(\mathbf{k} + \mathbf{q}) \cdot \boldsymbol{\Gamma}\} \{i\omega - \frac{k^2}{2m'} + \mathbf{d}(\mathbf{k}) \cdot \boldsymbol{\Gamma}\}}{\left\{ - \left(i\omega - \frac{(\mathbf{k}+\mathbf{q})^2}{2m'}\right)^2 + |d(\mathbf{k} + \mathbf{q})|^2 \right\} \left\{ - \left(i\omega - \frac{k^2}{2m'}\right)^2 + |d(\mathbf{k})|^2 \right\}} \right. \\ & \left. - \frac{\{i\omega - \frac{k^2}{2m'} + \mathbf{d}(\mathbf{k}) \cdot \boldsymbol{\Gamma}\} \{i\omega + \frac{k^2}{2m'} + \mathbf{d}(\mathbf{k}) \cdot \boldsymbol{\Gamma}\}}{\left\{ - \left(i\omega - \frac{k^2}{2m'}\right)^2 + |d(\mathbf{k})|^2 \right\} \left\{ - \left(i\omega + \frac{k^2}{2m'}\right)^2 + |d(\mathbf{k})|^2 \right\}} \right]. \end{aligned} \quad (\text{B5})$$

The first term, after expanding in small  $q$ , gives

$$t_1 \propto -e^4 \int d^d k \frac{3 m q^2 \sin^2 \theta}{4 k^8}, \quad (\text{B6})$$

which does not produce a log divergent correction to the Coulomb line. The second term can be written as:

$$\begin{aligned} t_2 & \propto e^4 \int \frac{d\omega d^d k}{k^2 |\mathbf{k} - \mathbf{q}|^2} \frac{\{i\omega - \frac{k^2}{2m'} + \mathbf{d}(\mathbf{k}) \cdot \boldsymbol{\Gamma}\} \{i\omega + \frac{k^2}{2m'} + \mathbf{d}(\mathbf{k}) \cdot \boldsymbol{\Gamma}\}}{\left\{ - \left(i\omega - \frac{k^2}{2m'}\right)^2 + |d(\mathbf{k})|^2 \right\} \left\{ - \left(i\omega + \frac{k^2}{2m'}\right)^2 + |d(\mathbf{k})|^2 \right\}} \\ & \propto e^4 \int \frac{d\omega d^d k}{k^2 |\mathbf{k} - \mathbf{q}|^2} \frac{-\omega^2 + \frac{k^4(m'^2 - m^2)}{4m^2 m'^2}}{\left(\omega^2 + \frac{k^4(m'^2 - m^2)}{4m^2 m'^2}\right)^2 + \frac{\omega^2 k^4}{m'^2}} \propto -e^4 m' \int \frac{dk}{k^{5-d} |\mathbf{k} - \mathbf{q}|^2}, \end{aligned} \quad (\text{B7})$$

which again does not produce a log divergent correction to the Coulomb line.

- 
- [1] A. A. Abrikosov, JETP **39**, 709 (1974), <http://www.jetp.ac.ru/cgi-bin/e/index/e/39/4/p709?a=list>.
- [2] E.-G. Moon, C. Xu, Y. B. Kim, and L. Balents, *Phys. Rev. Lett.* **111**, 206401 (2013).
- [3] L. Janssen and I. F. Herbut, *Phys. Rev. B* **92**, 045117 (2015).
- [4] I. F. Herbut and L. Janssen, *Phys. Rev. Lett.* **113**, 106401 (2014).
- [5] L. Janssen and I. F. Herbut, *Phys. Rev. B* **95**, 075101 (2017).
- [6] T. Kondo, M. Nakayama, R. Chen, J. J. Ishikawa, E. G. Moon, T. Yamamoto, Y. Ota, W. Malaeb, H. Kanai, Y. Nakashima, Y. Ishida, R. Yoshida, H. Yamamoto, M. Matsunami, S. Kimura, N. Inami, K. Ono, H. Kumigashira, S. Nakatsuji, L. Balents, and S. Shin, *Nat Commun* **6** (2015).

- [7] H.-H. Lai, B. Roy, and P. Goswami, ArXiv e-prints (2014), [arXiv:1409.8675 \[cond-mat.str-el\]](#).
- [8] R. M. Nandkishore and S. A. Parameswaran, [Phys. Rev. B \*\*95\*\*, 205106 \(2017\)](#).
- [9] D. Dalidovich and S.-S. Lee, [Phys. Rev. B \*\*88\*\*, 245106 \(2013\)](#).
- [10] I. Mandal and S.-S. Lee, [Phys. Rev. B \*\*92\*\*, 035141 \(2015\)](#); I. Mandal, [The European Physical Journal \*\*B 89\*\*, 278 \(2016\)](#); [Phys. Rev. B \*\*94\*\*, 115138 \(2016\)](#).
- [11] R. Shankar, [Rev. Mod. Phys. \*\*66\*\*, 129 \(1994\)](#).
- [12] O. Vafek and K. Yang, [Phys. Rev. B \*\*81\*\*, 041401 \(2010\)](#).
- [13] R. Nandkishore and L. Levitov, [Phys. Rev. B \*\*82\*\*, 115431 \(2010\)](#).